Macromolecular Bioscience
www.mbs-journal.de

Drug Delivery Systems for Photodynamic Therapy: The Potentiality and Versatility of Electrospun Nanofibers

Sofia M. Costa, Raul Fangueiro, and Diana P. Ferreira*

Recently, photodynamic therapy (PDT) has become a promising approach for the treatment of a broad range of diseases, including oncological and infectious diseases. This minimally invasive and localized therapy is based on the production of reactive oxygen species able to destroy cancer cells and inactivate pathogens by combining the use of photosensitizers (PSs), light, and molecular oxygen. To overcome the drawbacks of drug systemic administration, drug delivery systems (DDS) can be used to carrier the PSs, allowing higher therapeutic efficacy and minimal toxicological effects. Polymeric nanofibers produced by electrospinning emerged as powerful platforms for drug delivery applications. Electrospun nanofibers exhibit outstanding characteristics, such as large surface-area-to-volume ratio associated with high drug loading, high porosity, flexibility, ability to incorporate and release a wide variety of therapeutic agents, biocompatibility, and biodegradability. Due to the versatility of this technique, fibers with different morphologies and functionalities, including drug release profile can be produced. The possibility of scalability makes electrospinning even more attractive for the development of DDS. This review aims to explore and show an up to date of the huge potential of electrospun nanofibers as DDS for different PDT applications and discuss the opportunities and challenges in this field.

1. Introduction

Photodynamic therapy (PDT) has emerged as a promising treatment for several oncological and nononcological diseases, due to its minimal invasiveness and intrinsic selectivity, which derives from both the accumulation of drug in targeted site and the localized irradiation of lesions, providing a spatially and temporally selective cytotoxicity. Although photodynamic effect was discovered more than a century ago, its clinical application is relatively recent, only started to be widely used after the 1970s.[1,2]

S. M. Costa, R. Fangueiro, D. P. Ferreira
Centre for Textile Science and Technology (2C2T)
University of Minho
Guimarães 4800-058, Portugal
E-mail: sofiamcosta@det.uminho.pt
R. Fangueiro
Department of Mechanical Engineering
University of Minho
Guimarães 4800-058, Portugal

The ORCID identification number(s) for the author(s) of this article can be found under https://doi.org/10.1002/mabi.202100512

DOI: 10.1002/mabi.202100512

This therapy involves the administration of photoactive molecules, called photosensitizers (PSs), light, and molecular oxygen present in tissues. These three compounds are harmless individually, however, when combined they produce reactive oxygen species (ROS), such as singlet oxygen ($^1O_2{}^*$), hydrogen peroxide (H_2O_2), superoxide ion ($O_2{}^{\bullet-}$), or hydroxyl radical ($OH^\bullet$), which induce the death of target cells via oxidative damage.[3,4] After the intravenous, intraperitoneal, or topical administration of PS and its uptake by the target tissue, light of an appropriate wavelength is required to excite the PS, enabling the production of highly cytotoxic species, which will promote cell structural and functional failure.[5,6]

Over the years, PDT has been mainly used for cancer treatment including skin cancer, lung, esophagus, among others.[7] With more than 19.3 million new cases and 10.0 million deaths in 2020, cancer still represents one of the main causes of death worldwide.[8] Despite ongoing efforts in fundamental research and clinical practices to improve the effectiveness of cancer's prevention, diagnosis, and treatment, the high mortality rate for most cancers remains a challenge.[9,10]

During cancer progression, the tumor becomes highly heterogeneous, being composed by a mixed population of cells that present different molecular features and, consequently, different response to therapy. Moreover, the heterogeneity among patients and the ability of cancer cells to adapt and survive treatment becomes an obstacle to the conventional therapies.[9,11] Radiotherapy, surgery, and chemotherapy are the most common treatments for cancer in clinics, being the last one the most predominant therapeutic strategy. Chemotherapy as a systemic therapy, allows the treatment of tumors at any anatomical site in the body, which is especially important when metastasis occurs. However, its therapeutic potential is limited and far from satisfactory due to lack of tumor selectivity, poor drug bioavailability, high-dose requirements, development of multiple drug resistance, and serious side effects to healthy tissues, being the latter the major reason behind the high mortality rate of cancer patients.[12,13]

The low invasiveness, localized nature, fewer adverse effects, good patient tolerance, repeatability in the same area several times, and lower costs make PDT a promising alternative to classic therapeutic strategies.[7] Furthermore, the combination of PDT with other treatments has demonstrated a synergetic

antitumor effect, offering new opportunities for cancer therapy.[14] As PSs are fluorescent, they can be used for both diagnosis to identify malignant tissues as well as for therapy to treat the disease, acting as a theranostic agent.[15]

Although it is commonly used for cancer therapy, PDT has shown wide versatility and is also being explored to treat a variety of infectious diseases. The photodynamic effect was already demonstrated against bacteria, fungi, viruses, and parasites. Nowadays, one of the main concerns regarding the treatment of infections is the increase of microbial resistance to the conventional antimicrobials, due to their dissemination in the environment, and excessive or inadequate prescriptions. Therefore, there is an urgent need to discovery new therapies to combat infections, without developing microbial resistance. PDT also offers advantages in this field as it is a multitarget mechanism, which means that the produced ROS will affect multiple targets within microbial cells, instead of working on a one-target principle, which generally happens with conventional antimicrobials.[16–18]

Despite the tremendous potential of this therapy, most PSs present some drawbacks that limit its photodynamic effect and the clinical use of several molecules, namely significant dose requirements to achieve a consistent uptake by the target cells, which can result in prolonged and inappropriate photosensitivity, low PS solubility which favors its aggregation, possibility of degradation before reaching the target tissue, lack of biocompatibility, and also difficulty in reaching deep tissues.[19,20]

Drug delivery systems (DDS) are an effective approach to address these problems, being the focus of extensive research over the years. DDS aims to incorporate a therapeutic agent within the body, enhancing its efficacy and safety by controlling the rate, time period, and site of release, while decreasing the side effects.[21,22] In fact, drug encapsulation into DDS provides the protection of the drug from degradation in the bloodstream, better drug solubility, enhanced drug stability, targeted drug delivery, decreased adverse side effects, and improved pharmacokinetic and pharmacodynamic drug properties.[13] The advancements in nanotechnology and polymer science created innovative solutions for drug delivery. Nanostructures can act as DDS by encapsulating or attaching drugs and deliver them to target tissues, more precisely with a controlled release.[23]

Among nanocarriers, polymeric nanofibers synthetized by electrospinning have emerged as a promising solution due to their remarkable characteristics, which include high surface-area-to-volume ratio associated with high drug loading capacity, high porosity with interconnectivity, possibility to incorporate a wide range of molecules including insoluble drugs, possibility to control the drug release profile, good mechanical properties, a wide selection of the matrix materials, biocompatibility, and biodegradability. In fact, the use of natural or synthetic biodegradable polymers, able to be degraded into nontoxic monomers inside the body, for the development of electrospun nanofibers is crucial to avoid a secondary operation to dislodge the implanted carrier, as well as to allow an effective drug release.[22,24–26] These nanostructures are suitable for topical, transdermal, and oral drug delivery, and also for localized implantation onto the tumor tissue through imaging system-aided positioning via minimally invasive surgery or directly in tumor site after removal surgery.[25,27]

Regarding the treatment of infections, the structure of electropsun nanofibers is very advantageous, as it can mimic the extracellular matrix (ECM) structure, which favors the regeneration of skin in the wound area. The adaptability of these nanofibers to wound contour, the controlled delivery of therapeutic agents, and the possibility for gaseous exchange are other advantages of using these structures as DDS to treat wound-associated infections.[28,29]

Therefore, combining the intrinsic selectivity of PDT with the high drug loading capacity as well as the controlled drug release achieved by using electrospun nanofibers, the development of DDS based on biodegradable nanofibers loaded with PSs is a promising therapeutic approach to act locally, selectively and for a suitable time period, maintaining an appropriate drug amount at target site for the required time. Despite the advantages of nanofibers as DDS, and PDT as a therapy, being well studied, the combination of both is rather poor explored. Moreover, the use of biodegradable polymers to produce these DDS based on nanofibers is also very advantageous for PDT applications. Thus, this review aims not only to demonstrate the great potential of PDT to treat different diseases, and the capacity and versatility of electrospun nanofibers to act as DDS, but also to bring an updated overview and new insights about the combination of biodegradable nanofibers to carry the PSs for different PDT applications. To the authors' best knowledge, this is the first review exploring the combination of electrospun nanofibers for PDT, particularly for the treatment of cancer and infections, focusing on the use of biodegradable polymers.

2. Photodynamic Therapy

PDT is a clinical procedure used for the treatment of different malignant and nonmalignant diseases, which presents several advantages, like high accuracy, minimal invasiveness, controllability, low toxicity, and repeatable treatment.[30]

The concept of PDT was first reported by the works performed by Oscar Raab, Hermann von Tappeiner, and Albert Jesionek. In 1900, Oscar Raab observed that certain dyes could kill microorganisms when exposed to light. After this discovery, his professor Herman von Tappeiner together with the dermatologist Jesionek, found that the topical application of eosin followed by light exposure could treat skin tumors. In 1907, Jodlbauer and von Tappeiner demonstrated the necessity of the presence of oxygen for this light-mediated cytotoxicity, introducing the term "photodynamic action" to describe this phenomenon. The potential of PDT for cancer therapy was highlighted by the experiments performed by Thomas Dougherty and his colleagues. The first studies reported the potential of combining hematoporphyrin derivatives (HpD) and its activation with red light, in suppressing tumors in mice. Afterward, these experiments were performed in humans, which showed very successful results for the treatment of squamous cell carcinomas, basal cell carcinomas, and malignant melanomas, and the metastatic skin lesions.[31]

Curiously, 100 years after the discovery of photodynamic effect on killing microorganisms, this therapy has been mainly investigated for the treatment of several cancers. More recently, and due to the rising of multidrug resistance among pathogenic microbes, PDT has been explored for nonmalignant diseases, including antimicrobial applications.[32] In fact, this

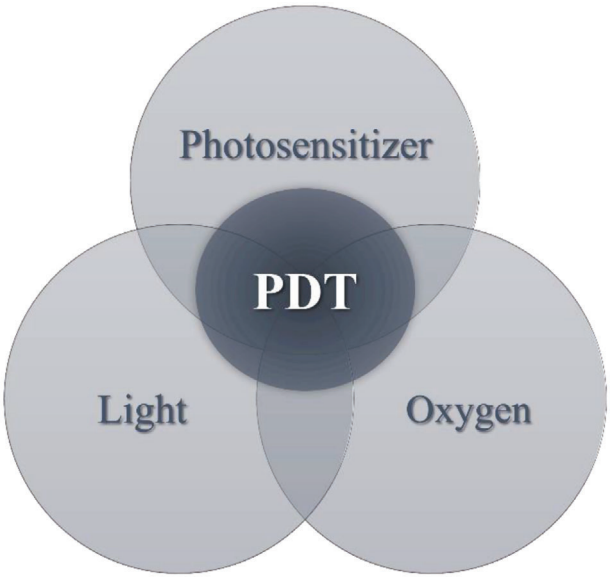

Figure 1. Combination of the three components required to achieve photodynamic effect. Adapted under terms of the CC-BY license.[1] Copyright 2021, the Author(s). Published by MDPI.

therapy has shown a great potential in various fields, like dermatologic (acne, psoriasis, etc.), ophthalmologic (central serous chorioretinopathy, age-related macular degeneration, etc.), cardiovascular (atherosclerosis, etc.), neurologic (Alzheimer's disease, etc.), dental diseases (periodontitis, etc.), among others.[33] Recently, few reports already start to explore the potential of PDT against COVID-19 pandemic caused by severe acute respiratory syndrome coronavirus 2 (SARS-CoV-2) virus, demonstrating once again the versatility of this therapy to treat a wide range of pathologies.[34–36]

PDT presents several advantages when compared to conventional treatments, including fewer long-term side effects, less invasiveness, higher selectivity, shorter treatment time, lower costs, and it can be applied at the same region multiple times without severe tissue damage (unlike radiation). However, the dependence on accurate light delivery to the tumor for treatment efficacy, the need for tissue oxygenation, the photosensitivity after treatment, and the impossibility to treat metastases are some of the limitations of this therapy.[7] For antimicrobial applications, PDT is commonly referred as antimicrobial PDT (aPDT), and also offers several advantages, such as a broad spectrum of action compared to antibiotics as PS can act on diverse organisms, less probability of developing resistance following multiple sessions of therapy, bactericidal effects independent of antibiotic resistance pattern, and more limited adverse effects.[37]

2.1. Mechanisms Underlying Photodynamic Therapy

PDT relies on the administration of a PS, which after a certain time interval (drug-to-light interval), is activated by light of appropriate wavelength on the target region in the presence of oxygen (**Figure 1**). This will lead to the generation ROS, which are highly toxic to the cells where the PS accumulated and light was delivered, showing the localized feature of this therapy.[38]

The Perrin–Jablonski diagram, representing the different processes leading to the production of ROS responsible for cell death, including $^1O_2{}^*$, is shown in **Figure 2**. Upon light irradiation with a specific wavelength, the PS goes from a ground state (S_0) to an excited singlet state (S_1), in which an electron shifts to a higher energy orbital without changing its spin. In this excited singlet state S_1, the PS is not able to participate in reactions with cellular substrates since this state presents very short lifetime (ns). From this unstable and short-lived state, the PS can return to its ground state S_0 by radiative energy in the form of light (fluorescence) or undergo nonradiative decay by releasing heat energy through internal conversion (IC). Alternatively, the PS can pass to a more stable and long-lived (µs) excited triplet state (T_1), via intersystem crossing (ISC), where the spin of the excited electron inverts. In this state, the PS can return to ground state S_0 by radiative (phosphorescence) or nonradiative processes (releasing energy in the form of heat).[3,7,39–41]

During PDT, the increased lifetime of the PS in this state allows the occurrence of photochemical reactions to produce reactive species, which are called Type I (electron transfer) and Type II (energy transfer) reactions. In Type I, the PS can react with nearby biomolecules (e.g., lipids, proteins, and nucleic acids) by transferring an electron or a proton to form anion radicals or cation species, respectively, which will further react with oxygen to generate ROS (superoxide, hydrogen peroxide, and hydroxyl radicals). In Type II reactions, the PS in its excited triplet state transfers energy directly to molecular oxygen in its triplet ground state ($^3O_2$), which leads to the production of $^1O_2{}^*$, a highly reactive and cytotoxic species. The lifetime of $^1O_2{}^*$ is very short (around 40 ns) and has maximum action radius of about 20 nm, which means that these species will only affect the substrates that are close to the local where they are formed, thereby to the site of photosensitization. These short lifetime and action radius together with the activation of the PS only in the irradiation area, makes PDT a very specific, controllable, and localized treatment.[3,7,39–41] Although Type II reactions are considered the main mechanism for efficiency of PDT, both reactions can occur simultaneously, and their contribution depends on several parameters, namely, the PS chemical structure (including the redox potential) and the oxygen concentration.[40,41]

2.2. Mechanisms of Cytotoxicity Induced by Photodynamic Therapy

Cell/tissue destruction mediated by PDT is a multifactorial process that involves three main mechanisms, as shown in **Figure 3**.

First, the direct death of target cells triggered by the burst of ROS generation, which will react with biological molecules, such as lipids, proteins, and nucleic acids, culminating in cell death mainly through apoptosis, necrosis or autophagy.[40] Subcellular localization of PSs in different organelles (mitochondria, lysosomes, endoplasmic reticulum, etc.) is a key factor to determine the cell death mechanism, since the site of $^1O_2{}^*$ production will almost certainly be the site of oxidative damage due to its reduced lifetime and action radius. A relationship between the intracellular localization of PS, and therefore, the induction of different cell death mechanisms has been established as one of the main factors to determine PDT toxicity, rather than the amount of the

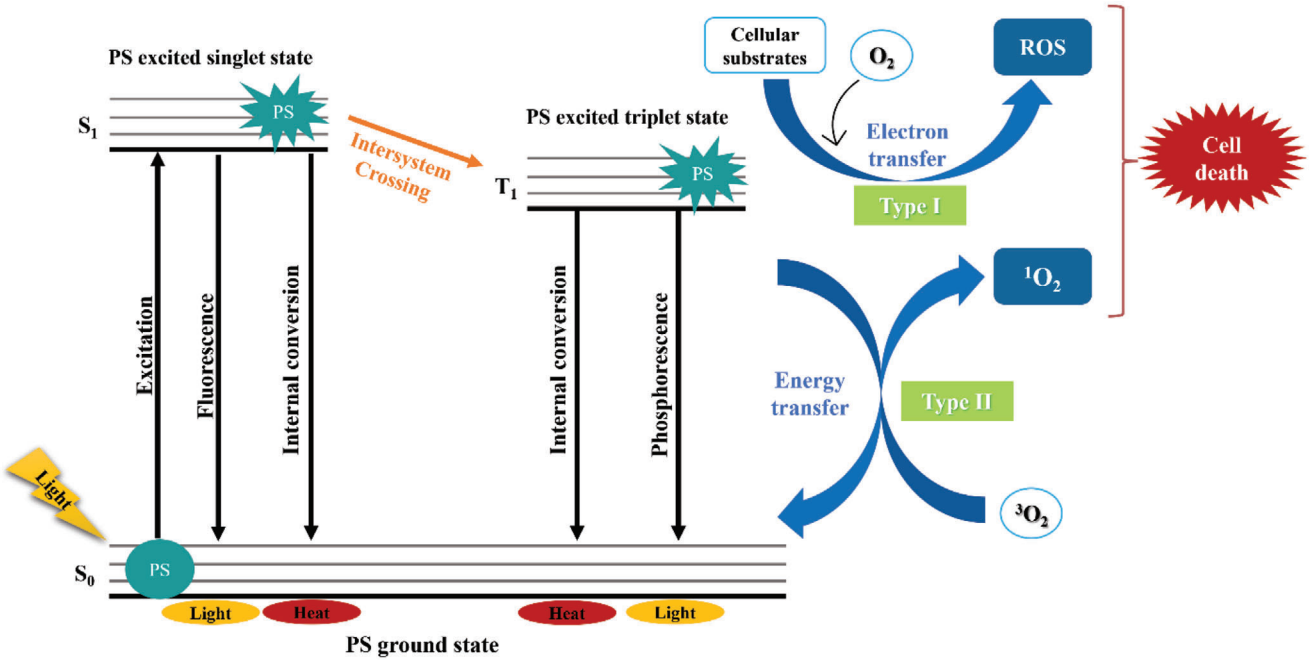

Figure 2. Perrin–Jablonski diagram representing the principles of PDT. Adapted under terms of the CC-BY license.[1,33] Copyright 2021, the Author(s). Published by MDPI.

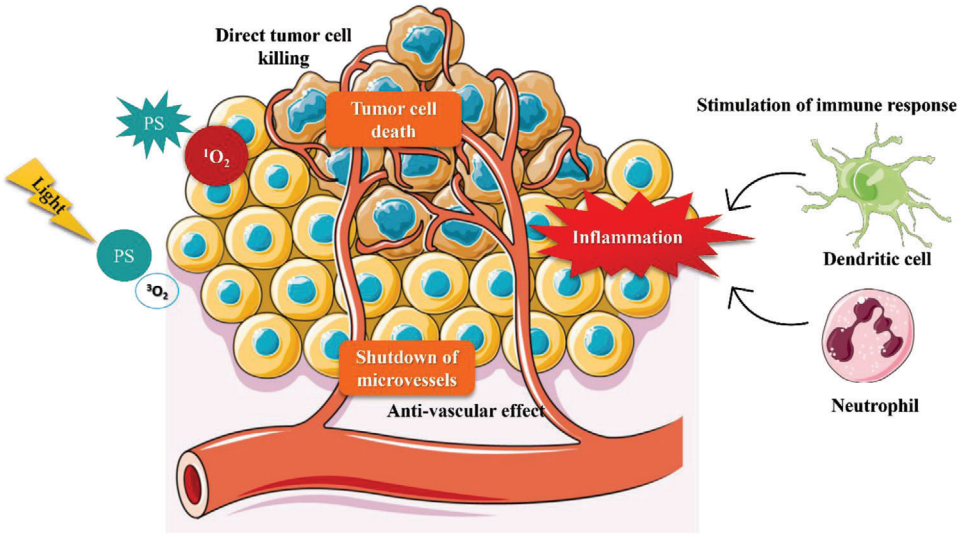

Figure 3. Illustration of the three mechanisms responsible for tumor destruction induced by PDT: direct tumor killing, antivascular effect, and stimulation of immune response. Created with smart.servier.com. Adapted with permission.[40] Copyright 2018, The Royal Society of Chemistry.

PS's uptake by the cells and the amount of $^1O_2{}^*$ generated.[40,42,43] The intracellular localization of the PS is largely governed by its chemical nature, such as its charge and amphiphilicity.[42,44] Besides the type, structure, dose and intracellular localization of the PS, the PDT outcome also depends on the cell type and illumination conditions.[44,45]

Second, the damage and shutdown of the vasculature that supplies the tumor. The microvessels are responsible for supply oxygen and nutrients that support the survival of tumor cells. Thus, the damage to these vessels can cause a decrease of the blood flow and tissue hypoxia, promoting cancer cell death.[46] However, it should be noted that if the microvasculature's shutdown is too sudden, leading to an abrupt drop in oxygenation, it can constitute an obstacle for PDT efficiency, since this therapy depends on having sufficient oxygen available.[40]

Third, the triggering of an acute inflammatory reaction in the targeted site can activate the innate immune system that will carry out the removal of damaged cells. After PDT-induced oxidative stress and traumatic insult, several proinflammatory mediators as well as damage-associated molecular patterns (DAMPs),

which act as signals for innate immunity, are released. The innate immune cells (monocytes or macrophages, neutrophils, and dendritic cells [DCs]) are recruited to the targeted site to attack the damaged cells. Moreover, the adaptive immune system may also be activated, resulting in the protection of the host organism in an antigen-specific manner, owing to immunological memory. PDT-mediated infiltration neutrophils also seems to have a crucial role in the elimination of invading bacteria, which is important to treat bacterial infections.[47]

2.3. Photosensitizers

As previously mentioned, apart from light source and tissue oxygenation, the type of PS has a strong impact in photodynamic effect. Over the last years, enormous efforts have been made for the development of more effective PSs. PSs are molecules that contain a chromophore, which absorb light at a specific wavelength with a high molecular absorption coefficient. These molecules can be obtained naturally or artificially, and the choice of the suitable PS is one of the critical factors for the PDT efficacy.[48] It should be noted that the ideal structure of the PS varies depending on the application.[32]

For cancer treatment, an ideal PS must have certain features to promote a better photodynamic effect, such as high purity, chemical stability, water solubility, high quantum yield (Φ_Δ) of $^1O_2{}^*$ generation, and strong absorption in the near-infrared (NIR) region (600–900 nm). In this region, which is called "phototherapeutic window," tissue light scattering is reduced allowing deeper penetration of light into tissues. The energy of the triplet state must be relatively high to promote the reaction with molecular oxygen. Moreover, the PSs should exhibit lack of toxicity in dark conditions, tumor selectivity, rapid accumulation in cancer cells, and rapid clearance from the patient's body to avoid post-treatment phototoxicity.[19,20,49] For antimicrobial applications, it is well established that cationic PSs are more effective against bacteria than anionic ones. As bacteria have negative charge on their surfaces, cationic PSs carrying a positive charge on their functional groups, can easily bound to and taken up by bacteria, enhancing the photodynamic effect.[37]

2.3.1. First-Generation Photosensitizers

The first-generation of PSs includes the HpD, obtained by purification and chemical modification of the first porphyrin used as PS—hematoporphyrin (Hp), which started to be utilized in the 1970s. Afterward, a mixture of porphyrin dimers and oligomers isolated from HpD, called Photofrin, was marketed. Their relatively high quantum yields for the production of ROS is one of the main advantages of these compounds for PDT applications. However, these PSs present some drawbacks, like low chemical purity, poor tissue penetration due to the limited absorption capacity above 600 nm, and long-term skin photosensitivity due to the excessive PS accumulation into the skin. Despite the disadvantages, HpD and Photofrin, are still widely used in clinics as PSs for the treatment of several cancers. Since mostly PSs commercially available are derived from porphyrins, extensive academic research has been focusing on the discovery and development of new compounds with improved characteristics, resulting in the so-called second generation.[39,41,50]

2.3.2. Second-Generation Photosensitizers

The second-generation PSs present various advantages over the first-generation ones, namely higher chemical purity, higher yield of $^1O_2$* formation, better penetration to deep tissues due to their maximum absorption in the NIR range. Furthermore, appropriate structural modifications in the PSs can contribute to enhance the photodynamic effect. For example, the introduction of heavy atoms into the PS potentially enhances the $^1O_2{}^*$ generation. This class of PSs includes chlorins, bacteriochlorin analogues, phthalocyanines, cyanines, squaraines, etc. Nevertheless, these PSs show poor solubility in water, which leads to a tendency to aggregate under physiological conditions, reducing the yield of ROS production, and it is also a limiting factor for their intravenous administration.[6,41,51,52]

2.3.3. Third-Generation Photosensitizers

As previously mentioned, most of the PSs do not display tumor tissue selectivity, being nonselectively distributed in the body, which can cause side effects.[53] The third-generation of PSs arises with the aim of providing new targeting treatment strategies, resulting in better therapeutic outcomes while reducing the adverse effects to healthy tissues. It is based on modified second-generation PSs to improve their pharmacokinetics and accumulation in the targeted cells. There are two main strategies to design and develop this class of PSs. The first one is based on the conjugation of the PS with a target moiety, such as carbohydrate molecules, antibody, or cell-penetrating or subcellular targeting peptides. The second approach is by the encapsulation of PS into DDS/carriers, like liposomes, micelles, nanoparticles, electrospun nanofibers, among others.[28,54]

3. Drug Delivery Systems as Photosensitizers' Carriers

The success of PDT can be limited by several factors, including the difficulty in the administration of some PSs, since most of them present low water solubility and stability. Thus, the use of DDS to carry the PSs can be advantageous in the improvement of the delivery efficiency, as well as to allow a spatiotemporally controlled release of the drug.[50]

In fact, the incorporation of PSs into surfaces offers several advantages, namely a decrease in the amount of PS to be administered, an increase of PS bioavailability, PS protection from degradation before achieving the target, loading and release of water-insoluble molecules, prevention of PS aggregation, promotion of the molecules rigidification by diminishing the photoisomerization process and also other deactivation mechanisms, and possibility to achieve a controlled and prolonged release of PS, which allows a constant and uniform concentration into target cells, minimizing the side effects.[19,20,25]

Nanotechnology-based DDS are attracting rising attention to be applied as diagnostic tools or to deliver therapeutic agents to

specific targeted sites in a controlled manner. With the rapidly progression of nanomedicine, advancements in the design of DDS either for their targeting to a particular location or for the controlled release of therapeutic agents at a particular site have been widely investigated. The green chemistry route to synthesize these DDS is also acquiring more and more importance since it minimizes the use of hazardous constituents, which can decrease the side effects of medications and also improve the sustainability of the processes.[23]

Polymeric micelles, liposomes, carbon-based materials, metal-based nanomaterials, upconversion nanoparticles (UCNPs), and nanogels are some examples of different nanocarriers studied all over the years. More recently, nanofibers produced by electrospinning using biodegradable and biocompatible polymers has been highly recognized as a potential candidate for drug delivery applications due to their outstanding features.[33,55] These nanofibers are particularly advantageous for localized drug delivery, allowing on-site delivery of drugs, reducing systemic toxicities and side effects to healthy cells.[56]

3.1. Electrospun Nanofibers as Drug Delivery Systems

Electrospun nanofibers have demonstrated great potential as DDS to be used for wound dressing, anticancer therapeutics, surgical implants, antibacterial systems, etc. These structures offer unique properties, including: i) large surface-area-to-volume ratio, which facilitates loading of high amount of drugs into these fibers; ii) high encapsulation efficiency; iii) physical structure that mimics the ECM, thus supporting cell adhesion, proliferation, migration and differentiation; iv) possibility for the loading and release of insoluble drugs; v) flexibility; vi) wide selection of the matrix materials; vii) vast possibilities for surface functionalization, which allows target-specific drug delivery; viii) high porosity with interconnected pore structure, which promotes cell adhesion, proliferation, drug delivery, and mass transport properties; ix) uniformity in fiber size; x) introduction of distinct bioactive molecules, which promote the development of multifunctional nanoplatforms able to meet different requirements; xi) ability to incorporate different combinations of drugs with simultaneous or sequential release kinetics.[25,27,57–60]

These structures are also a very promising implantable platform for in situ treatment, enabling a localized drug delivery, thereby minimizing the side effects to normal tissues and, at the same time, maximizing the drug action by favoring a controlled and sustained release directly at the site of action.[25,55] When using biodegradable materials to develop these DDS, the necessity of a removing surgery is no longer needed.[24] Furthermore, the implantation of DDS based on nanofibers at the post-surgical cavity after tumor resection, already proved to be more effective in prevent tumor recurrence when compared to systemic administration.[61]

By changing the fiber composition and fiber assembly structural parameters (e.g., fiber diameters, porosity, pore sizes, fiber's alignment, etc.), it is possible to have a local delivery of the bioactive agent with a controlled kinetics.[62]

The ability of nanofibers to support in vitro cell growth associated with their potential to control drug release, make these fibrous systems very suitable for drug delivery in several applications. The possibility to manipulate the composition and structure of nanofibers highlights their versatility to adapt and respond to different requirements, opening unlimited possibilities for personalized medicine.[63] In fact, electrospun nanofibers can provide different drug release profiles, including immediate, prolonged, biphasic and stimulus-activated release, which can be controlled according to the desirable application, being this subject explored in the following sections.[64] Therefore, electrospun nanofibers can amplify the therapeutic efficacy and potency of loaded PSs, while decreasing the undesirable side effects, by ensuring the accumulation of the PS in the target site and controlling its release, decrease the PS dosage, prevent PS aggregation, protect the PS from degradation in the body prior to arrival at the target tissue, increase PS bioavailability and by the possibility to incorporate and deliver different agents, including insoluble drugs.[25,60,65]

The localized nature of PDT together with great properties of electrospun nanofibers to act as localized DDS, make this approach very attractive and with strong potential. The exploration of the role of biodegradable electrospun nanofibers in PDT field, opens new possibilities to achieve a higher therapeutic efficacy with minimal side effects.

4. Electrospinning

Several methods have been used for producing fibers with diameters ranging from micrometers to nanometers. However, electrospinning is the most established technique for their production, due to its simplicity of use, accuracy, cost-effectiveness, versatility, and scalability. The ability to develop micro/nanofibers with different morphologies, patterns, and functionalities, using a variety of materials (e.g., polymers, ceramics, and metals), make this technique very attractive for a wide range of applications.[66] As previously discussed, electrospun nanofibers exhibit unique properties, making them suitable candidates for DDS. This section will explore the potential electrospinning technique and all the parameters that affect the production, morphology, and properties of electrospun nanofibers as well as their potential as DDS for the treatment of cancer and wound-associated infections.

Although the effect of the electrical charge on a liquid droplet dates to the 17th century by the work of A. D. William Gilbert, who put forward the concept of "electrospinning," the first patent describing the apparatus for producing artificial fibers using an electrical field was only published in 1934 by Anton Formhals.[67,68] Later, in 1969, Geoffrey Taylor reported that under an electrical field, the droplet emerged at the tip of the capillary tube acquired a conical shape and the fine jet came out from the vertices of the cone. This characteristic conical shape of the jet is now commonly referred as "Taylor cone."[67,69] In the following 20 years, electrospinning did not attracted considerable attention, until 1990, when Darrell Reneker and Gregory Rutledge reinvented and promoted electrospinning technology by confirming that a variety of polymers could be electrospun to produce fibers, thereby starting a new era of development of fibers on nanoscale.[68]

Over the years, electrospinning started to receive increasing attention not only within the scientific community, but also in industries, due to its great potential for responding to all major global challenges, including drug delivery, sensing, water and air

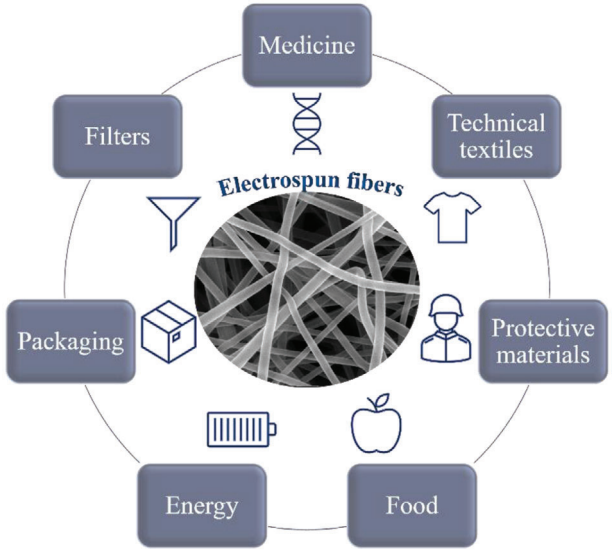

Figure 4. Different areas of application of micro/nanofibers produced by electrospinning. Adapted with permission.[55] Copyright 2021, Elsevier.

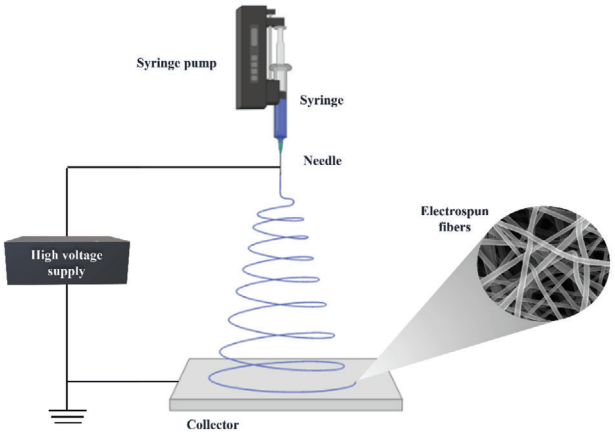

Figure 5. Schematic representation of a typical electrospinning setup. Created with BioRender.com. Adapted with permission.[74] Copyright 2019, Elsevier.

filtration, tissue engineering, food packaging, textiles, regenerative medicine, cancer therapy, wound healing, among other areas (**Figure 4**).[70–72]

Due to this wide range of applications, the number of publications as well as the investment related to electrospinning has increased through the years. The rising popularity and potential of electrospun fibers has led to great efforts to explore different approaches to scale-up the production, because the laboratory-scale electrospinning device with a single needle has a rather low (0.01–2 g h^{-1}) productivity.[73]

A typical electrospinning setup consists of a high-voltage power supply, a syringe with a metallic needle, a syringe pump and a conductive collector, as exemplified in **Figure 5**. Electrospinning principle is based on the formation of a jet when the liquid droplet is electrified, followed by its stretching and elongation to generate fibers. This process starts with the passage of polymer solution from the syringe to the needle to form a pendant droplet. When the electrical field is applied, the electrostatic repulsion among the surface charges stretches the droplet into a conical shape, known as Taylor cone. A charged liquid jet is ejected from the tip of Taylor cone, when the repulsive electric force overcomes the surface tension of polymeric droplet. Initially, the jet extends in a straight line and then undergoes vigorous whipping motions. The jet is continuously stretched, culminating in its deposition on a collector in form of solid fibers, accompanied with solvent evaporation.[24,71]

Modifications of the setup, namely, the spinneret geometry, allow the development of fibers with different morphologies and properties. Side-by-side, coaxial, and triaxial electrospinning are some of the examples that allow the production of fibers composed by two polymers placed one adjacent to the other, without physical mixing, core–shell fibers and fibers with three layers, respectively.[55] Needleless electrospinning or multichannel has also been attracting attention to achieve higher production rates, facilitating the large-scale production.[75]

Numerous compounds can be incorporated into electrospun nanofibers, such as natural extracts, nanoparticles, chemotherapeutic drugs, among others.[55,76] Several researchers have been exploring the use of electrospun nanofibers for cancer treatment, demonstrating promising results. For instance, Akpan et al. showed that the encapsulation of a chemotherapeutic drug into poly(lactic-*co*-glycolic acid) (PLGA)/gelatin nanofibers promoted a reduction in viability of two breast cancer cell lines, demonstrating the potential of these fibrous systems to act as a localized approach, reducing the toxicity to healthy tissues.[77] Electrospun nanofibers have also been studied as implantable for the treatment of several cancers, including brain tumors. Due to their high drug loading capacity, good stability and mechanical properties and sustained drug release, these nanofibers have shown tremendous potential as effective DDS to treat glioblastoma.[78] Other nanofibers' structures, like core–shell, have also been explored as a carrier of different drugs, to provide a more controlled and sustained release. Core–shell nanofibers already presented excellent efficacy as DDS for the in vitro local treatment of different cancer cells, including glioblastoma multiforme,[79] ovary,[80] melanoma skin,[81] breast cancer,[82] etc.

Electrospun nanofibers incorporated with different compounds, such as natural extracts, have also been reported as an excellent localized DDS for wound dressing applications. The biocompatibility and the prolonged drug release that can be achieved with nanofibers as well as their ability to act as a support for cell proliferation, make these fibrous systems very suitable to treat infections associated with wounds.[76,83] All of these research works demonstrate the potential of electrospun nanofibers to act as effective DDS for different applications.

4.1. Parameters Affecting the Electrospun Fibers' Morphology

The formation of electrospun fibers as well as their final morphologies and functionalities depends on several parameters, including the solution, process, and ambient conditions, which are discriminated in **Table 1**. The manipulation of these parameters enables the production of smooth, uniform, and beadless nanofibers, which is usually the desired outcome.[55]

Table 1. All the parameters (polymer solution, process and ambient) that affect the electrospun fiber's production, morphologies, and functionalities.

Polymer solution parameters	Process parameters	Ambient parameters
Polymer(s) molecular weight	Applied voltage	Relative humidity
Concentration	Feed rate	Temperature
Viscosity	Needle-to-collector distance	
Conductivity	Type of collector	
Surface tension	Needle diameter	
Solvent properties		

In fact, all of these conditions must be properly controlled and optimized to obtain the desirable morphology, as the membrane's morphology will affect their final properties, including the drug release. The correct optimization of these parameters is essential to achieve the highest quality of the final nanofibers for the desirable application. Despite being a simple technique to use, the proper adjustment of the various parameters can be a huge challenge and could require long time.[65,74]

4.1.1. Polymer Solution Parameters

The polymer molecular weight, polymer concentration, and solution viscosity are three important variables correlated with each other that can influence the final morphology of electrospun fibers. Solutions containing polymers of low molecular weight associated with lower viscosity tend to produce a mixture of beads and fibers with smaller diameters, when compared to solutions with polymers of high molecular weight at the same concentration.[84] The increase in polymer concentration is also associated with increased solution's viscosity, due to the increase in entanglement of the polymer chains,[76,83] and, consequently, in the formation of fibers with larger diameters and reduced defects.[85,86] Regarding the conductivity of the polymer solution, higher values promote a decrease in fibers' diameters due to the increase of charge density, resulting in stronger elongation forces in ejected jet.[87] It also favors a reduction of fibers' defects, decreasing the formation of beads.[88] The conductivity of polymer solutions can be determined by type of polymer, solvent, and the presence of salts.[89,90] During the electrospinning process, the electrostatic forces on the surface of the charged polymer solution need to overcome the surface tension to allow the ejection of the charged jet. Thus, higher surface tension values require stronger electrical field.[91] Generally, high surface tension promotes the formation of beads.[88,92,93] Solvent properties are also key factors affecting the fibers production and morphology. Solvent or solvent systems with higher conductivity and dielectric constant promote the formation of fibers with small diameters as well as the reduction of beads and nonuniform fibers.[94] Low volatile solvents presenting higher boiling point (lower vapor pressure) can be incompletely removed during the jet travelling course. The remaining solvent can redissolve and fuse the fibers, resulting in the production of thicker fibers.[95] Thus, volatile solvents are usually the preferred choice due to their rapid evaporation rate.[96] A mixture of different solvents is generally used to obtain fibers with the desirable properties.[94]

4.1.2. Process Parameters

A sufficient voltage able to overcome the surface tension of the polymer solution is required for the initiation of the jet.[97] The relationship between applied voltage and fibers' diameters is controversial. The rise in applied voltage was already demonstrated to reduce the fibers' diameters, and it is attributed to the increasing of electrostatic repulsion forces, resulting in greater stretching of the solution. The tendency to form beads was also reported.[98,99] On contrary, the increase in fibers' diameters with the increase of voltage was also reported by different works.[83,100,101] Regarding the feed rate, lower values are beneficial to maintain a balance between the leaving polymeric solution and replacement of that solution with a new one during jet formation.[86] On contrary, very elevated values of feed rate promote the formation of unstable jet and insufficient solvent evaporation, resulting in fibers with higher diameters and defects, and reduced deposition areas. Moreover, excessive values of feed rate can lead to the aggregation of polymer solution at the capillary tip.[83,85,102,103] A minimum distance is mandatory to give fibers enough time for drying prior to reaching the collector.[104] Generally, with the increase of distance between the needle and collector, the fibers' diameters decrease, as it allows a complete evaporation of the solvent and higher stretching of the jet.[105] Nevertheless, when this distance exceeds a certain value, the formation of beads as well as nonuniform and larger fibers occurs.[55,105] The internal diameter of the needle also plays an important role in the morphology of electrospun fibers. It has been shown that thinner and defect-free fibers with higher porosity are obtained using needles with small diameters.[106,107] The morphology of the fibers as well as their alignment are dependent on the design of the collector, which can be chosen according to the final application. Randomly or ordered aligned fibers and 3D structured fibers can be obtained using different collectors: static, rotating mandrel, rotating wire drum, guide wires, rotating disk, liquid bath collector, among others.[97] Ordered aligned fibers are obtained with rotating collectors, being the rotation speed a crucial factor to determine their final characteristics.[103,108]

4.1.3. Ambient Parameters

Ambient parameters, humidity and temperature, also affect the morphology of the fibers. The relative humidity during the electrospinning process influences the solvent evaporation rates as well as the porosity of the produced membrane. Generally, lower relative humidity values cause rapid solvent evaporation, resulting in thicker fibers, whereas higher relative humidity values cause slower solvent evaporation, which results in a decrease of fibers' diameters.[109] Nevertheless, some studies report an increase in fibers' diameters with the increase in relative humidity.[110] The surrounding temperature will not only affect the viscosity of the polymer solution but also the evaporation of the solvent.[111] Higher temperatures accelerate the solvent evaporation rate and promote a decrease in the solution's viscosity, resulting in higher stretching of the jet, and consequently, thinner

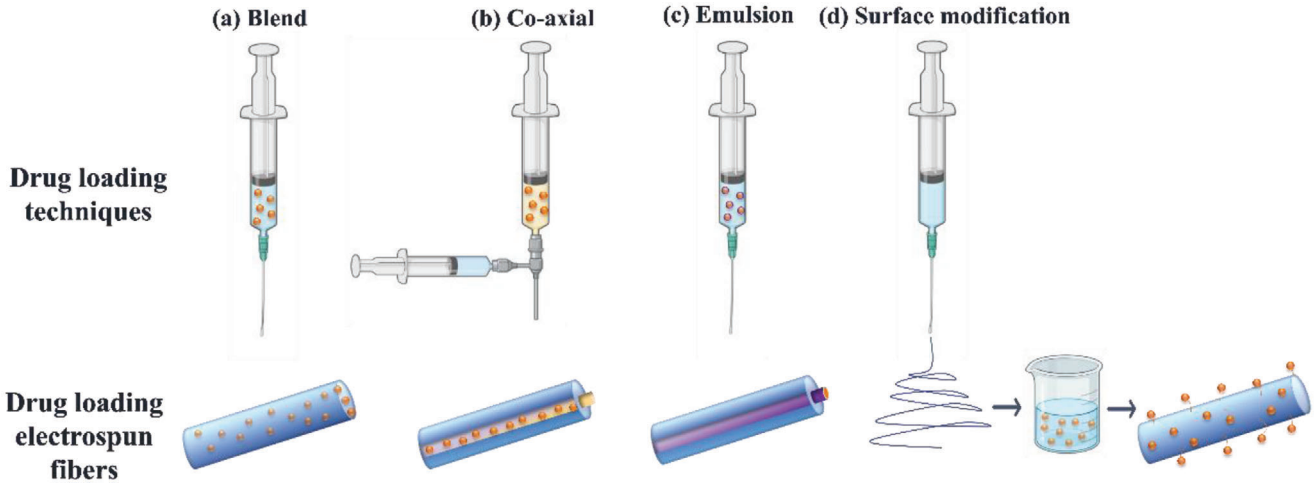

Figure 6. Drug loading by different electrospinning techniques: a) blend, b) coaxial, c) emulsion, and d) surface modification after the electrospinning process. Created with BioRender.com. Adapted with permission.[58] Copyright 2017, Elsevier.

fibers.[112] Nevertheless, exceeding a specific value of temperature leads to an increase in fiber's diameters. Despite most of the works are conducted at room temperature, there are some studies reporting the heating and maintaining of the working fluid at a constant temperature different from ambient condition during the electrospinning process.[113]

5. Biodegradable Polymers

Biodegradation is a term commonly used to describe the degradation of a material by the action of microorganisms (bacteria, fungi, algae, etc.). Nevertheless, for medical purposes, biodegradation refers to biological processes that occur inside the body, which leads to gradual degradation of the material.[114] This is especially important for drug delivery applications, since degradation of polymers inside the body is essential for effective drug release and to avoid surgical removal of the material at the end of its therapeutic lifetime. Furthermore, biodegradable polymers are nontoxic and cause lower inflammatory reactions.[24,115–117] Besides being biodegradable, the polymers used for medical applications should be biocompatible, nontoxic, nonmutagenic, nonimmunogenic and provide appropriate mechanical properties.[114,116]

Once the materials are inside the body, their physical and chemical properties can be changed, promoting their gradual degradation. Biodegradation can occur by mainly four general mechanisms, which include oxidation (due to oxidants produced by tissues), hydrolysis (reaction with water in tissues), enzymatic degradation and physical degradation (e.g., water swelling and mechanical loading and wearing).[24,114]

Biodegradable polymers are usually divided in two main categories: natural and synthetic. Natural polymers, which include chitosan, gelatin, cellulose, alginate, starch, etc., are produced by biological systems, such as microorganisms, plants, and animals. Besides their natural origin, these polymers are biocompatible and degrade into nontoxic, non-immunogenic components. On the other hand, synthetic polymers can be obtained by polymerization of monomers. Polylactic acid (PLA), polyethylene glycol (PEG), and poly(ε-caprolactone) (PCL) are some examples of synthetic polymers. Besides their biodegradation inside the body, these polymers are biocompatible, which is also a requirement for DDS applications.[115–117] Hence, the DDS's functional time, degradation rate as well as the formed products must be well-characterized and controlled for the success of a polymer implant.[24,116]

6. Drug Loading Techniques via Electrospinning

The incorporation of drugs into electrospun fibers can be carried out using different techniques. Besides the typical electrospinning method, also called as blend (or co-) electrospinning, there are also other electrospinning techniques that require different setups and allow the development of distinct nanofibers' structures. The drug loading procedure strongly influences the drug release profile. **Figure 6** shows the most common electrospinning techniques for drug loading, according to the spinneret configuration: blend (or co-), coaxial, emulsion, and surface immobilization technique.[55,118–120]

6.1. Blend Electrospinning

The blend (or co-) electrospinning is widely used to produce drug-loaded fibers and involves the conventional electrospinning setup, with a single syringe and a needle. In this case, drugs can be incorporated by dispersing or dissolving them with polymer solution prior to the electrospinning process, resulting in nanofibers with drugs dispersed throughout the fibers.[121,122] Several requirements must be considered, like the physicochemical properties of polymers as well as their interaction with drugs, as they will affect drug encapsulation efficiency, drug distribution, and drug release kinetics.[24] Nevertheless, this approach presents some drawbacks, including the possibility of denaturation of bioactive molecules and loss of biological activity in the presence of organic solvents used in the polymer

solution, the reduced encapsulation efficiency of the prepared fibers, the unequal distribution of drugs into the fibers and the burst release of the drug, which is generally observed using this methodology.[97,123]

6.2. Coaxial Electrospinning

Coaxial electrospinning is considered another drug loading methodology, being able to produce core–shell or hollow nanofibers. In fact, core–shell nanofibers composed by an inner and an outer compartment, denoted as core and shell, respectively, have been shown tremendous potential for biomedical applications, particularly for drug delivery. In this technique, a coaxial spinneret composed by two needles is used to simultaneously electrospun two different polymer solutions, resulting in the formation of core–shell fibers, in which each of them maintains their separate identities.[124,125] This method not only gives the possibility to use an infinite combination of polymers and benefits from the properties of each, but also offers one-single platform for the loading of different drugs in distinct compartments of the fibers. Moreover, the incorporation of a drug onto the core, which in turn will be coated by the shell, could effectively control the drug's release profile and protect the drug from damage, offering a great advantage to this type of structure.[55,126,127]

6.3. Emulsion Electrospinning

An alternative approach for the development of core–shell fibers is the emulsion electrospinning. Contrary to coaxial method, which requires the use of coaxial spinneret, emulsion electrospinning requires the same setup of blend electrospinning. This technique involves the simultaneous spinning of stable emulsion of two or more fluids, which are not mixed during the electrospinning process. Emulsions can be categorized in oil-in-water (O/W) and water-in-oil (W/O), where droplets of oil are dispersed in the continuous water phase, and aqueous droplets are dispersed in the oil phase, respectively. The substance responsible for the formation of the droplets in an emulsion is referred to as the "dispersed phase," whereas the surrounding liquid is called "continuous phase." The dispersed phase is converted into the core of fibers, while the continuous phase forms the shell layer. For example, W/O emulsion can be used to encapsulate hydrophilic bioactive molecules and the polymers used in this phase are water-soluble polymers. On the other hand, the polymers used in continuous phase are soluble in lipophilic solvents.[128,129] This will minimize the contact of bioactive molecules with organic solvents and allow the use of several combinations of hydrophilic drugs and hydrophobic polymers.[55,130]

6.4. Surface Immobilization/Modification

In surface immobilization method, the electrospun membranes are firstly produced, and then drugs are loaded onto the membranes by chemical (covalent bonding) or physical interactions (electrostatic interaction, van der Waals interaction, or hydrogen bonding). Due to the high surface-to-volume ratio of electrospun fibers, several adhesion sites exist to attach the drug molecules.[57] Most of the post-electrospinning methods only alter fiber surface, being the choice of the surface modification method dependent on the desirable fibers' final properties. Chemical adsorption, wet chemical techniques (aminolysis, hydrolysis, etc.), surface graft polymerization, and plasma treatment are some of the examples of chemical modification techniques, while simple physical adsorption and layer-by-layer (LBL) assembly are referred to physical modification techniques.[131,132] With this method, it is possible to overcome some of the difficulties associated with the conventional techniques, namely, to avoid the direct contact between the bioactive molecule with the organic solvent, which can prevent its degradation.[55] It could also improve the homogeneity, adhesion, and stability of the molecules at the fibers surface.[85]

7. Drug Release Profiles from Electrospun Fibers

The main aim of a DDS is to deliver a required amount of one or more drugs for a defined period of time according to the medical condition.[126] The knowledge of the conditions influencing the drug release profile is essential to design and develop a DDS with a suitable drug release, to achieve the desired therapeutic effect. Several factors strongly influence the release profiles of drugs, such as the fibers' fabrication method, processing conditions, drug loading method, polymer and bioactive agent physical-chemical properties, and the resulting fibrous structure and morphology.[55,62] The drug release from nanofibers can occur by different mechanisms, namely, desorption/dissolution of drug from the nanofiber surface, diffusion through the channels and pores of the polymer matrix, and erosion or degradation of the polymer matrix. In most cases, a combination of them occurs simultaneously.[21,24,59,133]

According to nanofibers' composition and structure, diverse drug release profiles can be achieved: immediate, modified-release (prolonged or biphasic [fast followed by slow release]), and stimulus-activated drug release, as shown in **Figure 7**.

The immediate release corresponds to the rapid release of the drug to achieve the pharmacological effects within minutes after its administration. A suitable polymer, high surface-to-volume ratio, which provides a large contact area for dissolution, and high porosity of the nanofiber membrane are exploited to achieve immediate drug release.[64]

Although the burst release could be required under certain circumstances,[134] in most of the cases, the initial burst release is undesirable because it shortens the duration of the drug's therapeutic effect, which may not ensure the healing efficacy, and may even cause toxicity.[135]

To overcome this unpredictable and uncontrolled release, several research works have been focusing on the investigation and development of innovative modifications and alternatives to decrease the burst release, and at the same time, to achieve a more controlled and prolonged release profile.[57] The controlled and sustained drug release results in enhanced product safety as well as improved treatment efficacy.[136] The use of biodegradable or swellable polymers that degrade gradually in a controlled manner and/or that swell in a biological environment is very promising to develop drug-loaded nanofibers with prolonged drug release.[64]

Despite electrospun fibers produced by blend electrospinning are generally associated with a burst release, they can

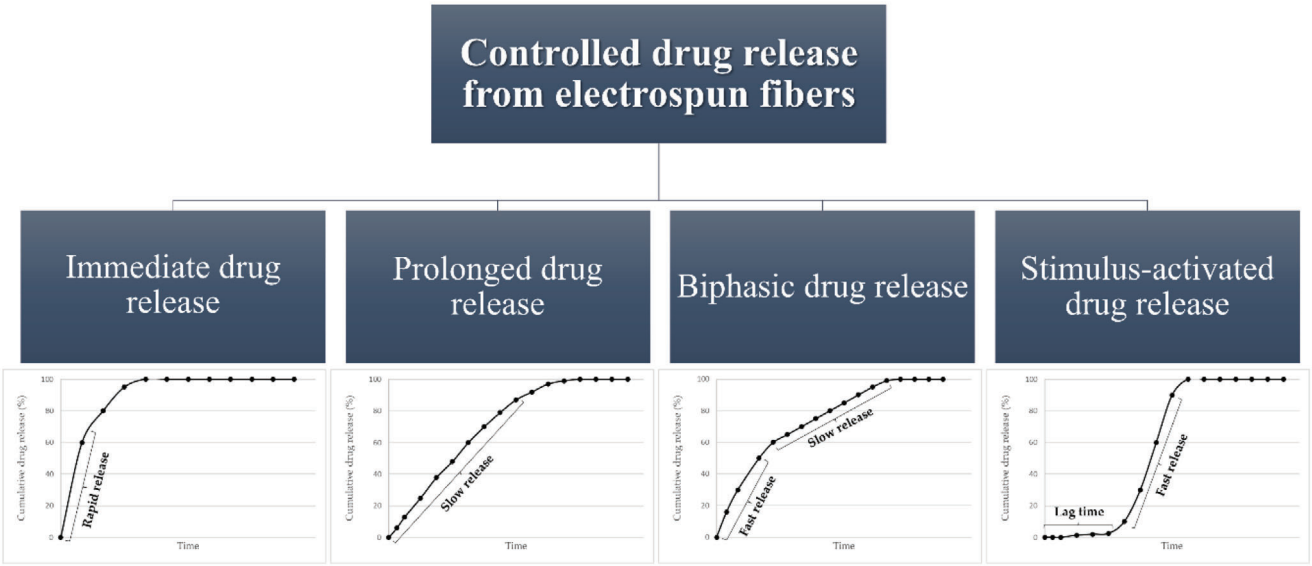

Figure 7. Classification of electrospun fibers based on their drug release profile: immediate, prolonged, biphasic and stimulus-activated drug release. Adapted with permission.[64] Copyright 2019, Elsevier.

also be good candidates to provide a more prolonged drug release.[76,133,137] Ribeiro et al. developed antimicrobial electrospun membranes based on biodegradable polymers, chitosan/PEO/cellulose nanocrystals (CNC), incorporated with acacia natural extract to act as a localized DDS for wound dressing applications. A continuous release of the acacia extract from the nanofibers to the solution was observed for 24 h, confirming the prolonged effect of the nanofiber's membranes containing the natural extract at least over a day, as demonstrated in **Figure 8**.[76]

Blends of PLGA/poly(ethylene glycol)-*b*-poly(D,L-lactide) (PEG-*b*-PDLLA) incorporated with ciprofloxacin hydrochloride (CiH) demonstrated three stages of drug release: Stage I exhibited a short duration and was controlled by fiber swelling and diffusion according to Fick's second law; Stage II exhibited long duration and slow release rate and was controlled by diffusion through a fused membrane structure; most of the drug was released in Stage III with a large release rate and was controlled by polymer degradation. Blending PLGA with different second polymers could regulate the hydrophilicity and degradation rate of the matrix, changing the drug release behavior of CiH.[133]

Ramachandran et al. predicted and prepared nanofiber implants based on PLGA-PLA-PCL loaded with an anti-glioma drug, Temozolamide (TMZ). The nanofiber implants were developed by simultaneously spinning three different polymer-drug blends onto a single target, using a co-electrospinning unit loaded with multiple cartridges, which resulted in a 3D wafer containing various nanofibers capable of releasing the drug for specific periods. One combination provided a sustained and prolonged drug release for 30 d in a challenging tissue microenvironment like brain tumor, which was extremely relevant for controlling tumor growth and prohibiting tumor recurrence in orthotopic brain tumor models, resulting in long-term (>4 month) survival of 85.7% animals.[137]

Core–shell nanofibers have been demonstrated to be a suitable strategy to provide prolonged drug release. Typically, the drug is loaded onto the core, which is surrendered by a shell layer, that will act as a rate-controlling barrier for drug release.[64] Moreover, the possibility to incorporate in one-step multidrugs simultaneously in each layer may open a wide range of applications, as it is possible to create a time-programmed DDS with sequentially release of each drug. This will allow to achieve the effect of each drug at the adequate time using the same DDS.[138] It also offers the possibility to incorporate both soluble and insoluble drugs in the same nanocarrier.[139] Thus, these types of structures will moderate the initial burst release and enable a sustained drug release for a longer time, thereby maximizing the duration of drug effect.[126]

Several studies already demonstrated the potential of core–shell nanofibers in providing a more sustained release profile compared to their simple blended counterparts produced by co-electrospinning.[59,79,140–142] Huang et al. found that core–shell nanofibers composed by collagen and a hydrophilic drug, berberine chloride (BC), into the core, and poly-L-lactic acid (PLLA) into the shell provided a long-term release compared to monolithic PLLA nanofibers in alkaline conditions. The fast drug release from monolithic PLLA was due to the quick dissolution of the BC deposited on the surface, following penetration of water into the vacant pore of the dissolute drug to enhance the matrix hydrolysis. On the other hand, core–shell nanofibers provided a controllable long-term release, which could be induced by diffusion and slow degradation of the shell, being the complete release achieved after 192 h. **Figure 9** shows the proposed drug release mechanism from monolithic and core–shell nanofibers.[59]

Alishahi et al. showed that the core–shell structures were able to reduce the initial burst release and prolong the release for 9 h, whereas almost all the loaded drug was released after 5 h when using single blended nanofibers.[140] Another research work also demonstrated the ability of core–shell to decrease the initial burst release obtained with blended nanofibers. Besides showing the influence of electrospun fibers' structure on drug release profile,

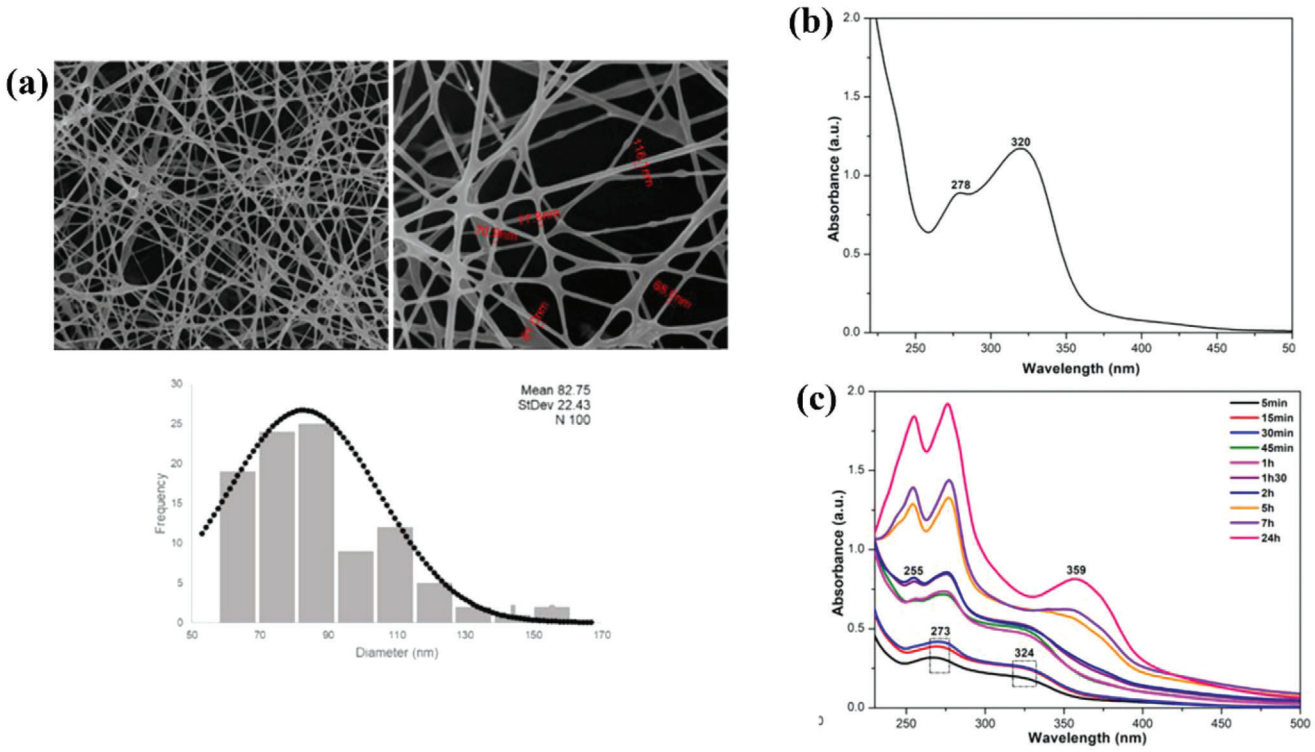

Figure 8. a) FESEM images of chitosan/PEO/CNC nanofibers incorporated with 6 mg mL^{-1} of acacia extract and diameter distribution histogram. Acacia's release profile: b) absorption spectra of the pseudo-extracellular fluid (PECF) solution containing acacia and c) release profile of the acacia extract from the nanofiber membrane to the solution for a period of 24 h. Reproduced with permission.[76] Copyright 2020, Elsevier.

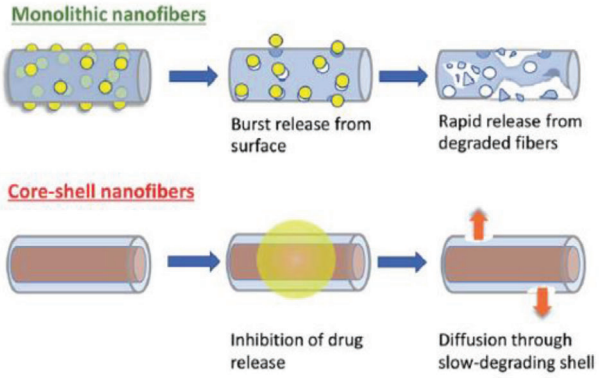

Figure 9. Schematic representation of the proposed drug release from PLLA monolithic fibers and collagen/PLLA core–shell nanofibers. Reproduced under terms of the CC-BY license.[59] Copyright 2021, the Author(s). Published by The Royal Society of Chemistry.

the authors also demonstrated that the composition of the shell layer as well as the concentration of the drug have an effect on this parameter.[141] The thickness of the shell layer also plays an important role in drug release.[79]

In the work performed by Abudula et al., core–shell fibrous structures composed by chitin-lignin in the core, and PCL in the shell, prevented the burst release of methylene blue (MB) observed in both hybrid and PCL fibers (**Figure 10**). The drug release from core–shell was directly proportional to the dissolution rate of the core fiber layer, and the PCL shell layer contributed to prolong the drug release. Core–shell structures loaded with penicillin/streptomycin also exhibited a superior inhibition effect against *Escherichia coli* (*E. coli*) and *Staphylococcus aureus* (*S. aureus*) bacteria, compared to simple nanofibers. These results show their greater inhibitory potential against bacterial strains by maintaining a controlled and localized release of the therapeutic agents.[142]

Other suitable strategy is the development of tri-layer nanofibers by triaxial electrospinning, which showed to provide a better drug dual-stage release profiles than traditional core–shell nanofibers. The addition of a middle layer in tri-layer nanofibers acted as a diffusion barrier able to manipulate the drug diffusion rate from the core to the bulk dissolution media, keeping an accurate amount of first-stage drug release and a longer sustained release in the second stage.[143] The sandwich geometry of nanofiber mats also demonstrated to be an effective configuration for delaying the release of drugs.[144] Different post-treatment can also be adopted to delay the drug release, such as the crosslinking.[145]

Nanofibers can further act as stimuli-responsive nanocarriers, also called smart systems, since they can enhance/trigger the release of drugs in response to a specific stimulus, resulting in the controlled release of therapeutic molecules in a spatial and temporal manner. The stimuli able to trigger the release of the drugs can be either endogenous (pH, oxidative stress, enzymes, temperature, carbohydrates, chemicals) or exogenous (heat, magnetic field, ultrasound, light, electric field).[146]

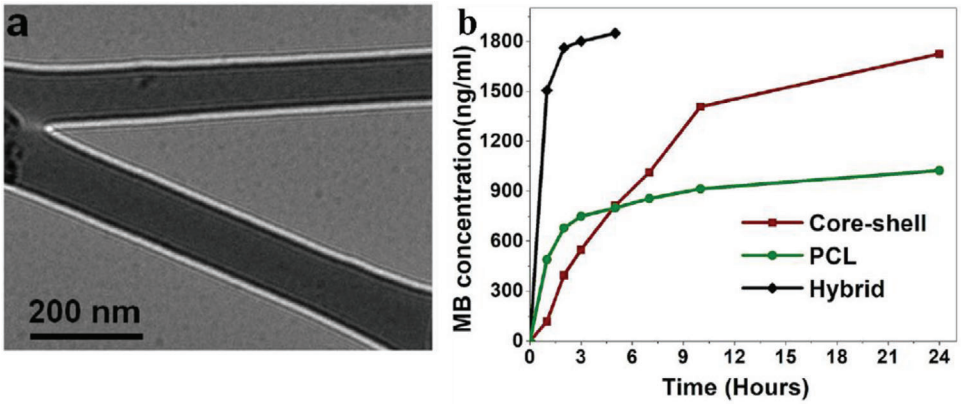

Figure 10. a) TEM image of the core–shell fiber; b) MB release profile from the electrospun scaffolds. Reproduced under terms of the CC-BY license.[142] Copyright 2020, the Author(s). Published by Springer Nature.

Table 2. A summary of electrospun systems based on biodegradable polymers for cancer PDT.

Biodegradable electrospun system	PS	Light source, wavelength, power/power density/energy density, and irradiation time	Drug release time	Application	Ref.
PLLA	Purpurin-18	Diode laser light 702 nm 10 mW	N/A	Human hepatocellular carcinoma cell line (SMMC-7721) and human esophageal cancer cell line (ECA-109)	[147]
PLLA/PEO	5,10,15,20-tetrakis (4-carboxyphenyl) porphyrin (TCPP)	Laser 532 nm 100 mW cm^{-2} 30 min	72 h	Human cancer cells (HeLa cells)	[148]
Chitosan/PEO	Photosens	Laser 100 mW cm^{-2} 15 min	96 h	Noncancerous (MC3T3-E1 murine osteoblasts) and cancerous [T-47D (mammary gland)] cell line	[149]

N/A = Not applicable.

8. Biodegradable Electrospun Nanofibers as Drug Delivery Systems for Photodynamic Therapy Applications

The combination of electrospun nanofibers as DDS composed by biodegradable polymers and containing PS shows great potential to treat a wide range of pathologies, including cancer and infections, using the photodynamic effect. This section will explore the different research works reporting the use of biodegradable electrospun fibers for the treatment of cancer and infections using PDT. It will also describe how different parameters (nanofibrous systems, type and concentration of PS, power/energy, irradiation time, etc.) will affect the PDT outcome.

8.1. Cancer Treatment

Being cancer one of the leading causes of death worldwide, the need to explore novel strategies to enhance the efficiency of cancer therapy, while minimize its side effects, and thereby improving the patient's life quality is crucial.[9] Despite the described potential of combining electrospun nanofibers with PSs, only few studies report their use for cancer PDT applications, as shown in **Table 2**.

Wu et al. developed PLLA electrospun nanofibers containing the PS purpurin-18. The results showed that both human hepatocellular carcinoma cell line (SMMC-7721) and human esophageal cancer cell line (ECA-109) were able to adhere and spread on the surface of the PLLA-purpurin-18 nanofibers, demonstrating the good biocompatibility and absence of toxicity of these nanostructures. Finally, a reduction in the survival rate of both cell lines after exposure to irradiation was observed, demonstrating that these cells could be killed through PDT. Nevertheless, without irradiation, the survival percentage of ECA-109 cells was very low.[147]

Ma et al. developed electrospun nanofibers of PLLA/PEO polymers containing 5,10,15,20-tetrakis(4-carboxyphenyl) porphyrin (TCPP) as PS. A burst release of PS was observed during the first 7 h, and sustained release thereafter until 72 h. On contrary to the previous study, TCPP-loaded PLLA/PEO nanofibers showed low dark toxicity on human cancer cells (HeLa cells) while promoted their death after exposure to radiation, showing the killing of cancer cells by PDT. These nanofibers also exhibited good biocompatibility, demonstrating the huge potential of PS-loaded nanofibers to act as DDS for cancer PDT.[148]

Besides testing the photoactive effect on cancerous cells, Severyukhina et al. also evaluated the effect on noncancerous

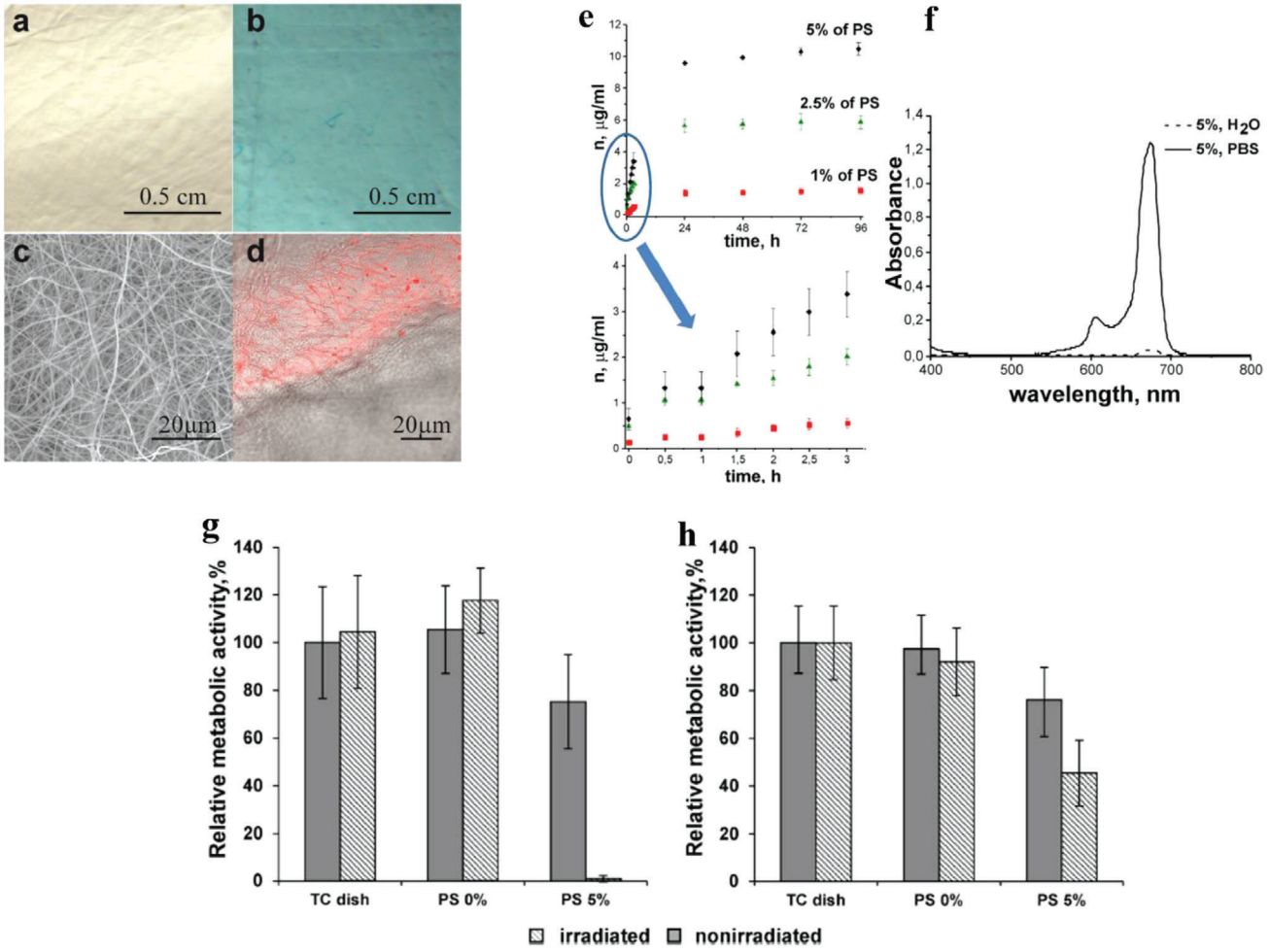

Figure 11. Photographs of electrospun membranes: a) without PS and b) with 5% of PS. c) SEM image and d) overlay of transmission bright field and confocal fluorescence images of electrospun fibers with 5% of PS. e) Release profile from electrospun membranes loaded with different concentrations of PS in PBS within 96 h, with a inset showing the release during the first 3 h. f) Absorbance spectra of the supernatant liquids after 96 h of PS release from the fibers loaded with 5% PS in water and in PBS. Joint effect of irradiation and of the scaffold loaded with 5% PS on the temporal dynamics of cellular metabolic activity: g) T-47D cells and h) MC3T3-E1 cells grown for 24 h before irradiation and grown for a further 24 h after it. Reproduced with permission.[149] Copyright 2016, Elsevier.

ones.[149] Chitosan and PEO biodegradable polymers were used to produce nanofibers combined with PS second generation, with strong absorbance in the NIR region. The developed membranes are shown in **Figure 11**a–d. The PS release was studied for 96 h and occurred in two stages: a burst release during the first 24 h, related to the release of physically adsorbed PS during the swelling of the fibers, and a sustained release thereafter resulted from the slow dissociation of the chitosan–PS complexes (Figure 11e). Moreover, the amount of released PS not only increased with increasing PS content in the nanofibers, but also was higher in PBS (pH 7.4) when compared to distilled water (pH 5.5) (Figure 11f). The effect of the developed nanofibers on cancerous (T-47D breast cancer cells) and noncancerous (MC3T3-E1 murine osteoblasts) cells was evaluated. The authors observed that the dark toxicity of the nanofibers was variable according to PS content. For lower PS concentrations, the cellular metabolism was unaffected, while the samples with higher PS amount induced a slight metabolic inhibition. This was observed for T-47D cancerous cell line, where nanofibers with 2.5% and 5% PS induced a reduction in their metabolic activity, whereas MC3T3-E1 noncancerous cell line was unaffected by the PS in the nanofibers, even when it was used at the highest concentration of 5%. Otherwise, the exposure to radiation promoted a significant reduction in the metabolic activity (>90%) of cancerous cells, while osteoblasts were resistant to photodynamic effect, highlighting the preferential phototoxic effect on malignant tissues (Figure 11g,h).[149]

PS-loaded nanofibers also demonstrated to be a great approach to cover stents, thereby improving their efficacy to treat tumors.[150] For instance, the efficacy of the implantation of a drug-eluting stent covered by electrospun fibers containing albumin-chlorin e6-manganese dioxide nanoparticles (ACM NPs) at the injured area was evaluated using an orthotopic rabbit oesophageal cancer model. ACM stents were able to produce O_2 in the presence of tumoral endogenous H_2O_2, alleviating the hypoxic microenvironment within the tumor. O_2 generation

capability of ACM NPs contributed to enhance the photodynamic effect and to increase the survival rate of animals, demonstrating to be an effective therapeutic approach to eliminate local solid tumors.[151]

The use of core–shell nanofibers is poorly explored for cancer PDT applications. Nevertheless, these structures already demonstrated to be efficient in providing a more controlled and prolonged release of different agents, including chemotherapeutic drugs, antibiotics, among others.[25,79,141] Thus, it is also expected that core–shell nanofibers show less burst release in initial stages while promoting a prolonged release of encapsulated PSs than single nanofibers for cancer PDT.

8.2. Infection's Treatment

The use of PDT to prevent and/or treat infections associated with wounds, contributing significantly to accelerate the wound healing process, has been the focus of several research works. Because of the large number of drug-resistance microorganisms, this therapy arises as a very promising and advanced alternative to antibiotics. Commonly referred as aPDT, this treatment can effectively kill bacteria, viruses and fungi locally, reducing the damage to normal tissues and with low probability of creating antimicrobial resistance.[152]

Considering all the advantages of electrospun nanofibers to act as a DDS, their use as a platform to carry the PS could be a very suitable approach to treat wound associated infections. As previously mentioned, the structure of nanofibers mats is able to mimic the ECM, acting as a support for cell proliferation, thereby promoting the skin regeneration, which is required to enhance the healing process. The highly interconnected porosity not only allows gases to pass through the dressing and reach the wound site, preventing desiccation and dehydration, but also hinders the penetration of microorganisms. Besides being able to incorporate and delivery drugs for a long time and sustained manner, these ultrafine structures can easily adapt to the wound.[28,153] Ensuring a sustained drug release for this application is also important to reduce the frequency of dressing's replacement, and consequently, weaken or eliminate the injuries associated to that.[154]

Several studies already demonstrated the efficiency of PS-loaded nanofibers using biodegradable polymers to kill different bacteria responsible for several infections with photodynamic effect, as shown in **Table 3**.

For instance, Severyukhina et al. used chitosan and PEO biodegradable and biocompatible polymers with a second-generation PS to produce electrospun fibers, which displayed light-induced antibacterial activity against *S. aureus* bacteria.[17] Czapka et al. also evaluated the antibacterial properties of electrospun photoactive nanofibers against *S. aureus* bacteria. The developed cellulose acetate (CA) nanofibers embedded with MB, promoted a reduction in the number of *S. aureus* biofilm cells formed on the surface CA/MB nanofibers, which was dependent on the duration of exposure to light, being the most effective reduction equal to 99.99 ± 0.3% after 180 min of light irradiation.[155]

The work performed by Contreras et al. demonstrated the effect of PS-loaded nanofibers on Gram-negative bacteria using PCL or PLGA encapsulated with PSs (MB or erythrosin B [ER]). PCL scaffolds loaded with PSs were able to reduce the number of *E. coli* bacteria under radiation, being this effect more significant using MB-loading nanofibers in comparison with ER-encapsulated nanofibers. Moreover, it was observed that the longer the light exposure, 30, 60 and 120 min, the higher the log reductions of bacteria, 0.5, 0.9, and 1.8, respectively, when using PCL/MB nanofibers. This finding could be explained by the increased release of MB from the scaffold in comparison to ER, thereby an increase in cellular MB uptake is expected. Furthermore, considering the cationic nature of MB, a greater interaction with bacteria cell membranes is also expected.[156]

Contrary to the previous studies, Preis et al. evaluated the potential of PS-loaded nanofibers against both Gram-positive and Gram-negative bacteria. Indocyanine green (ICG) NIR dye was incorporated into PLA solution to produce PLA/ICG nanofibers to be used as a photoresponsive wound dressing. During the first 6 h a burst release of ICG was observed, followed by sustained release until 168 h. PLA/ICG nanofibers loaded with the higher ICG concentration showed a significant reduction of both Gram-positive and Gram-negative bacteria, which was dependent on the irradiation time. The greatest effects were obtained after 30 min of irradiation, where PLA/IGG nanofibers induced a reduction of 99.978% (3.66 $\log_{10}$), 99.699% (2.52 $\log_{10}$), and 99.977% (3.64 $\log_{10}$), for *S. saprophyticus*, *E. coli*, and *S. aureus*, respectively. The nanofibers showed good biocompatibility, providing a good support for cells to adhere and spread on the surface of the samples as well as to infiltrate the nanofibrous mesh and grow in multiple directions, and exhibited favorable proangiogenic effects.[157]

Jiang et al. also evaluated the aPDT of fibrous systems against both Gram-negative (*E. coli* K-12) and Gram-positive (*Bacillus subtilis*) bacteria. In this case, they synthetized photoactive benzo[c]-1,2,5-oxadiazole based conjugated microporous polymer nanoparticles (TBO NPs), which were added to polyvinyl alcohol (PVA) solution, resulting in PVA-TBO nanofibrous membranes by colloid electrospinning. These membranes were able to achieve 100% of cell death after 120 and 60 min of visible light irradiation against *E. coli* and *B. subtilis*, respectively. Moreover, without light irradiation, PVA-TBO membranes did not showed any cytotoxicity to bacteria cells. The antibiofilm properties of these membranes were further studied. In the presence of light, biofilm was not formed, while in the absence of light PVA-TBO membranes were not able to inhibit the formation of biofilm. These photoactive membranes also demonstrated good cytocompatibility.[158]

Porphyrin-conjugated regenerated cellulose (RC) nanofibers were produced by electrospinnig of CA, followed by thermal treatment of the electrospun membranes, and finally their hydrolyzation to produce RC nanofibers. Subsequently, the covalent grafting of protoporphyrin IX (PPIX) was performed using epichlorohydrin/triethylenetetramine (TETA), followed by zinc chelation (RC-TETA-PPIX-Zn). Using RC-TETA-PPIX membranes, antibacterial effect was detected for both bacteria, with detection limit inactivation (99.999%, 5 log units) achieved within 20 min of illumination for *S. aureus*, and a 99.994% (4.6 log units) reduction in CFU reached in 40 min for *E. coli*. On the other hand, using RC-TETA-PPIX-Zn nanofibers, both bacteria exhibited detection limit killing (99.999%, 5 log units) within 20 min. To assess the photostability, the antibacterial activity of "photo-aged" RC-TETA-PPIX-Zn nanofibers, which were pre-illumination

Table 3. A summary of electrospun systems based on biodegradable polymers for the treatment of infections by PDT.

Biodegradable electrospun system	PS	Light source, wavelength, power/power density/energy density, and irradiation time	Drug release time	Application	Ref.
Chitosan/PEO	Photosens	Light-emitting diode 675 nm 80 mW cm^{-2} 10 min	N/A	*S. aureus*	[17]
Cellulose acetate (CA)	MB	Neon tube 430 and 660 nm 30 W 30, 90, and 180 min	N/A	*S. aureus*	[155]
PCL or PLGA	MB or Erythrosin B (ER)	LED 30, 60, or 120 min	100 h	*E. coli*	[156]
PLA	Indocyanine green (ICG)	Weberneedle Endo Laser 810 nm 500 mW 5, 15, 30, and 60 min	168 h	*Staphylococcus saprophyticus* subsp. *bovis*, *E. coli* DH5 alpha and *S. aureus* subsp. *aureus*	[157]
Polyvinyl alcohol (PVA)	Benzo[c]-1,2,5-oxadiazole based conjugated microporous polymer nanoparticles (TBO NPs)	Visible light 460 nm 0.1 W cm^{-2}		*E. coli* K-12 and *Bacillus subtilis*	[158]
CA	Protoporphyrin IX (PPIX)	Xenon lamp 250 or 500 W 5, 10, 20, 40 min or 5 h	N/A	*S. aureus* and *E. coli*	[159]
Polyhydroxybutyrate (PHB)/PEG	MB	LED array 635 nm 150 mW In vitro: 100 J cm^{-2} In vivo: – days 0, 1, and 3: 100 J cm^{-2} for 25 min – days 7 and 8: 200 J cm^{-2} for 50 min	7 days	In vitro*: S. aureus* strain ATCC 6538P (SA_{st}) and Methicillin resistant *S. aureus* strain clinical isolate (MRSA) In vivo: SAst-inoculated excision wounds in immunocompromized rats	[160]
Chitosan/PVA	ICG	781 nm In vitro: – ICG solution: 60, 120, 180, 240, and 300 J cm^{-2} – Nanofibers: 120 J cm^{-2} for 4 min In vivo: 200 mW cm^{-2} for 20 min	96 h	In vitro: Methicillin-resistant *S. aureus* (MRSA) and Meropenem-*resistant Pseudomonas aeruginosa (MRPA)*. In vivo: rats with infected wounds with MRSA	[154]
Poly(γ-glutamic acid) (γ-PGA)	5,10,15,20-tetrakis(1-methylpyridinium-4-yl)porphyrin tetra (p-toluenesulfonate) (TMPyP)	3 mW cm^{-2} 30 and 60 min	N/A	In vitro*: S. aureus* and *E. Coli* In vivo*: S. aureus*-infected mice wound model	[161]
CA/PEO	MB	Light-emitting diode 635 nm In vitro: 5 or 10 min In vivo: 30 min	24 h	In vitro*: Pseudomonas aeruginosa, S. aureus, Klebsiella pneumoniae* In vivo: diabetic mouse model bearing infected skin wounds (*S. aureus* and *P. aeruginosa*)	[18]
PCL	RB@ZIF-8 NPs	Visible lamp 515 nm 1.8 mW cm^{-2} 15 and 30 min	N/A	In vitro*: S. aureus* and *E. coli* In vivo*: S. aureus*-infected mouse model	[162]
PCL/Polyvinylpyrrolidone (PVP)	Core–shell UCNPs@Curcumin	Laser 808 nm 20 min	N/A	In vitro: MRSA and *E. coli*	[163]
PCL/PVP	Core–shell UCNPs@hypericin	Laser 808 nm 0.5 W cm^{-2} 20 min	N/A	In vitro: MRSA In vivo: MRSA-infected wounds	[164]

N/A = Not applicable.

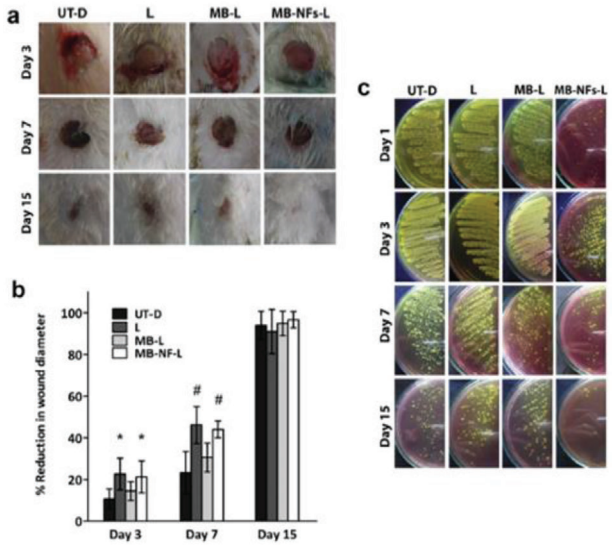

Figure 12. a) Morphological characteristics of excision infected wounds in different animal groups; b) time-course of percentage reduction in wound diameter. $*P < 0.05$, $\#P < 0.01$ versus untreated group at the same day of examination; c) degree of bacterial contamination of the wounds over a 15 d study period. UT-D: Untreated control rats kept in the dark; L: Control rats treated with red light; MB-L: Control rats treated with MB solution and red light; MB-NF-L: Rats treated with MB-eluting PHB/PEG NFs and red light. Reproduced with permission.[160] Copyright 2017, Elsevier.

during 5 h to simulate the effects of photobleaching, was evaluated, showing no statistically significant loss in antibacterial activity against either *S. aureus* or *E. coli* when compared to the pristine RC-TETA-PPIX-Zn nanofibers.[159]

The efficacy of PS alone when compared to PS-loaded nanofibers for aPDT applications was evaluated as well as the effect of these nanofibers on in vivo models. El-Khordagui et al. used polyhydroxybutyrate (PHB)/PEG polymers combined with MB as the PS. The developed nanofibers exhibited a biphasic drug release with an initial burst release followed by a sustained release for 7 d. The photoactivation of PHB/PEG/MB nanofibers showed to be more effectively in killing both *S. aureus* standard strain (SA_{st}) and methicillin resistant *S. aureus* strain clinical isolate (MRSA) bacteria than MB solution. One possible explanation may be due to the sequestration and accumulation of bacteria in nanofibers, which may facilitate the uptake of eluted MB by bacterial cells and localized $^1O_2{}^*$ generation. The authors also compared the effect of MB solution and PHB/PEG/MB nanofibers in vivo using a SA_{st}-inoculated excision wounds in an immunocompromized rat model. MB-containing nanofibers promoted a higher reduction of the wound diameter at day 7 as well as a greater bacterial killing by day 15, when compared to MB solution, as demonstrated in **Figure 12**. The superior healing potential of the PHB/PEG/MB nanofibers was also corroborated by histological analysis of the wound tissue, and by the decreased levels of tumor necrosis factor-α (TNF-α) in wounds treated with PHB/PEG/MB nanofibers, which is known to inhibit wound re-epithelialization with suppressed synthesis of ECM proteins.[160]

Qiu et al. also evaluated in vitro and in vivo the potential of chitosan/PVA/ICG nanofibers combined with photodynamic effect to treat infected wounds. These nanofibers were able to release 15% of ICG during the first 15 min, reaching the appropriate ICG concentration for bacteriostasis, and then a sustained release was observed for 96 h. ICG solution showed bacteriostatic effect against methicillin-resistant *S. aureus* (MRSA) and meropenem-resistant *Pseudomonas aeruginosa* (MRPA) under illumination, being this effect dependent on the ICG and irradiation doses. A better effect was observed in Gram-positive when compared to Gram-negative bacteria, which can be explained by different structures of bacterial cell walls. While the cell wall of Gram-positive is composed of porous peptidoglycan and phosphoric acid, allowing the passage of PSs, the Gram-negative presents an outer membrane composed of lipopolysaccharides, lipoproteins and lipid bilayers, which forms a permeability barrier that prevents the entry of PSs. Under light irradiation, chitosan/PVA/ICG nanofibers demonstrated a strong antibacterial effect against MRSA, showing that the release of ICG from nanofibers can exert an antimicrobial effect. Without illumination, these nanofibers also showed certain bacteriostatic effect, which can be attributed to chitosan itself. The effect of these electrospun membranes were also evaluated in vivo on rats with infected wounds with MRSA. On days 7 and 15 the number of bacteria colonies was smaller using ICG/chitosan/PVA nanofibers with illumination than the other treatment groups (model using sterilized gauze, positive control using Fucidin, chitosan/PVA nanofibers, ICG solution with illumination, ICG/chitosan/PVA nanofibers), demonstrating the higher antibacterial efficiency using nanofibers as a PS carrier when compared to ICG alone. On day 15, the skin structure was complete for this group, since the morphology of collagen was clear, and the arrangement was tight and orderly. Moreover, positive expression of cluster of differentiation 31 (CD31) in ICG/chitosan/PVA nanofiber with illumination on day 15 indicated the generation of a large number of new blood vessels, while the expression of the glycoprotein F4/80, a marker of macrophages, was reduced. Finally, on days 7 and 15, the levels of inflammatory cytokines, TNF-α and interleukin-6 (IL-6), in the rats of ICG/chitosan/PVA nanofiber group with illumination was the lowest. Overall, these results demonstrate the potential of PS-loaded nanofibers approach for the treatment of wound infections.[154]

Sun et al. used poly(γ-glutamic acid) (γ-PGA), a bacterially produced homo-polypeptide, which shows highly biocompatibility, biodegradable properties and minimal immunogenicity, and a cationic photosensitizer 5,10,15,20-tetrakis(1-methylpyridinium-4-yl)porphyrin tetra (p-toluenesulfonate) (TMPyP) to produce electrospun nanofibers for antibacterial PDT. In vitro results showed great effect on bacterial reduction of *S. aureus* and *E. coli* with γ-PGA-TMPyP nanofibrous mats after irradiation, being this effect proportional to TMPyP concentration and irradiation time. Once again, the antibacterial effect was more pronounced on Gram-positive when compared to Gram-negative bacteria. The in vivo evaluation in *S. aureus*-infected mice wound model revealed that γ-PGA-TMPyP mats when irradiated exhibited faster wound closure rates, reduced number of bacteria and less inflammatory cells, restraining the inflammatory reaction, thereby enhancing the wound healing process.[161]

Khalek et al. evaluated the synergetic effect of nanofibers loaded with MB and Ciprofloxacin (Cipro) antibiotic, using a diabetic mouse model bearing infected skin wounds. The group where the wound was covered with CA-PEO-MB nanofiber,

followed by irradiation, and then covered with CA-SF nanofiber, which consisted of tri-layered structure (CA-PEO; silk fibroin [SF]; CA-PEO) till the end of the treatment duration, achieved 80% of wound closure. The group where the wound was covered with CA-PEO-MB nanofiber, followed by irradiation, and then covered with CA-SF-Cipro nanofiber, which consisted of tri-layered structure (CA-PEO-Cipro; SF; CA-PEO-Cipro), showed 95% of wound closure, demonstrating a synergetic activity between photodynamic and antibiotic effects. This group also exhibited higher re-epithelization, collagen deposition and expression of CD34 and TGF-β while showed lower expression of pro-apoptotic CD95+ cells, in comparison with monotherapy, and the controls. Thus, the combination of PDT and antibiotic could be achieved by sequentially applying MB-loaded nanofibers then Cipro-loaded ones to the same wound, allowing to overcome drug–drug interaction problems reported in cases of coloading in the same dressing and to allow different administration times.[18]

The PSs can also be combined with other structures, such as metal–organic frameworks (MOFs), and then incorporated into electrospun fibers. Qian et al. encapsulated the PS rose bengal (RB) into zeolitic imidazolate framework-8 (ZIF-8) to obtain photodynamic antimicrobial RB@ZIF-8 NPs, which were incorporated into PCL solution to produce MOF-based mixed-matrix membranes (MMMs). The membranes exhibited excellent capability to generate ROS, resulting in significant antibacterial activities against *S. aureus* and *E. coli* under the visible light irradiation, being this effect more pronounced using higher RB@ZIF-8 NPs concentration and longer irradiation time. Once again, *E. coli* demonstrated better tolerance against ROS than Gram-positive bacteria. *S. aureus*-infected animals treated with PCL/RB@ZIF-8 nanofibers under irradiation, showed less purulent aspect, better skin regeneration, smaller rate of wound area, reduced bacteria colonies, and less inflammatory cells, demonstrating their potential to accelerate the wound healing. Additionally, these nanofibers presented good biocompatibility.[162]

Other possible approach is to combine the PS with UCNPs, which can convert NIR light into short-wavelength light, activating the surrounding PSs while allowing deeper penetration depth in tissue.[163] Zhang et al. synthesized core–shell structures composed by UPCNPs coated with hypericin as the PS, to be embedded into polyvinylpyrrolidone (PVP)/PCL nanofibers. Besides proving the efficiency of electrospun membranes against MRSA bacteria under NIR irradiation, being this effect more efficient with higher UCNPs@hypericin concentrations, the authors also demonstrated their potential to treat MRSA-infected wounds in vivo. Interestingly, the group treated with the fibers prepared by in situ electrospinning, where the fibers were directly deposited to the wound as they are produced, exhibited faster recovery than the group treated with the membranes produced by traditional electrospinning. This result can be due to the better adhesiveness on the skin by the fibers deposited directly onto the wound, which can more effectively prevent bacteria from entering the wound from the side-edge gap of the membrane and allows the ROS produced in the fiber to effectively reach bacteria in the wound, since these species have a short-range effect. In fact, in the in situ PDT group, the bacteria reduction rate was the fastest, and on the 16th day, the local tissues were clearly epithelialized contrary to the other groups.[164]

9. Conclusions

In the past few years, PDT has been recognized as a great potential therapy to treat a variety of diseases. Despite being well-known for the treatment of cancer, PDT has gained increasing attention to treat a wide range of clinical applications, including infections. The combined interaction of PS molecules, oxygen and light leads to the generation of ROS, which are able to destroy tumoral tissues and several pathogen agents (bacteria, fungi, viruses, etc.). Its minimal invasiveness and localized response make this therapy very attractive in clinics, namely, for treating different cancers and infections. The systemic administration of PSs offers several problems. The use of DDS to carry these molecules can be a promising approach to improve the therapy's efficiency.

Electrospinning has emerged as a potent technique to produce fibrous structures to act as drug delivery vehicles. The widely diversity and versatility in polymer matrix materials, drug loading techniques, fibers' morphologies and properties, drug release profiles and biological activity make electrospun fibers very suitable materials to act as DDS able to meet different specifications. Moreover, the simplicity, high efficiency, low cost, reproducibility, and possibility to be scaled up for an industrial level also make electrospinning a very attractive technology for the investment of the scientific community and industries.

Using electrospun nanofibers to incorporate and deliver the PSs can be a great strategy to act more locally and to promote a more controlled and prolonged drug release, thereby decreasing the side effects and improving the therapeutic efficacy. The use of biodegradable polymers to produce these nanofibers is very advantageous, as it allows an effective release of PS and avoids a secondary operation to remove the fibrous structure. Although the combination of electrospun nanofibers for PDT applications is underrepresented in research, some works already demonstrated the potential of this approach in vitro and in vivo. Despite all the overview presented in this review, there is still a lot to explore regarding the use of biodegradable nanofibers as DDS for PDT applications.

Thus, work needs to be done to better understand the mechanisms underlying the different sensitivity of cells to PDT, test different PSs, as well as to develop new nanofibers systems able to carry the PS, particularly for cancer PDT, evaluating the combination of different polymeric materials to achieve better outcomes, such as a controlled and sustained release profile of PS, suitable functional and degradation times of DDS, and a decrease of PS toxicity in the dark while an enhancement of its effect when irradiated. Moreover, the exploration of core–shell fibers for this application is crucial, as these structures present better results in retarding initial burst release and providing a sustained long-term drug release.

Acknowledgements

The authors are thankful to project UID/CTM/00264/2021 of 2C2T – Centro de Ciência e Tecnologia Têxtil, funded by National Founds through FCT/MCTES- Fundação para a Ciência e a Tecnologia. D.P.F. is thankful to CEECIND/02803/2017 and S.M.C. to the FCT PhD Scholarship (SFRH/BD/147517/2019), founded by National Founds through FCT/MCTES.

Conflict of Interest

The authors declare no conflict of interest.

Keywords

biodegradable polymers, cancer, drug delivery systems, electrospun nanofibers, infections, photodynamic therapy

Received: December 23, 2021
Revised: February 2, 2022
Published online: March 18, 2022

[1] A.-G. Niculescu, A. M. Grumezescu, *Appl. Sci.* **2021**, *11*, 3626.
[2] J.-J. Hu, Q. Lei, X.-Z. Zhang, *Prog. Mater. Sci.* **2020**, *114*, 100685.
[3] D. Van Straten, V. Mashayekhi, H. De Bruijn, S. Oliveira, D. Robinson, *Cancers* **2017**, *9*, 19.
[4] J. M. Dąbrowski, in *Inorganic Reaction Mechanisms*, Vol. 70 (Eds: R. van Eldik, C. D. Hubbard), Academic, San Diego, CA **2017**, Ch. 9.
[5] E. Lima, O. Ferreira, V. S. D. Gomes, A. O. Santos, R. E. Boto, J. R. Fernandes, P. Almeida, S. M. Silvestre, L. V. Reis, *Dyes Pigm.* **2019**, *167*, 98.
[6] S. Friães, E. Lima, R. E. Boto, D. Ferreira, J. R. Fernandes, L. F. V. Ferreira, A. M. Silva, L. V. Reis, *Appl. Sci.* **2019**, *9*, 5414.
[7] G. Calixto, J. Bernegossi, L. De Freitas, C. Fontana, M. Chorilli, *Molecules* **2016**, *21*, 342.
[8] W. H. Organisation, *Int. Agency Res. Cancer* **2020**, 13.
[9] C. Pucci, C. Martinelli, G. Ciofani, *Ecancermedicalscience* **2019**, *13*, 961.
[10] L. Poláková, J. Širc, R. Hobzová, A.-I. Cocârță, E. Heřmánková, *Int. J. Pharm.* **2019**, *558*, 268.
[11] P. Zhang, C. Hu, W. Ran, J. Meng, Q. Yin, Y. Li, *Theranostics* **2016**, *6*, 948.
[12] S. Shen, M. Liu, T. Li, S. Lin, R. Mo, *Biomater. Sci.* **2017**, *5*, 1367.
[13] S. Senapati, A. K. Mahanta, S. Kumar, P. Maiti, *Signal Transduct. Target. Ther.* **2018**, *3*, 7.
[14] Q. Zhang, L. Li, *J. BUON.* **2018**, *23*, 561.
[15] O. J. Klein, H. Yuan, N. H. Nowell, C. Kaittanis, L. Josephson, C. L. Evans, *Sci. Rep.* **2017**, *7*, 13375.
[16] A. Almeida, *Antibiotics* **2020**, *9*, 138.
[17] A. N. Severyukhina, N. V. Petrova, A. M. Yashchenok, D. N. Bratashov, K. Smuda, I. A. Mamonova, N. A. Yurasov, D. M. Puchinyan, R. Georgieva, H. Bäumler, A. Lapanje, D. A. Gorin, *Mater. Sci. Eng., C* **2017**, *70*, 311.
[18] M. A. Abdel Khalek, S. A. Abdel Gaber, R. A. El-Domany, M. A. El-Kemary, *Int. J. Biol. Macromol.* **2021**, *193*, 1752.
[19] D. P. Ferreira, D. S. Conceição, R. C. Calhelha, T. Sousa, R. Socoteanu, I. C. F. R. Ferreira, L. F. Vieira Ferreira, *Carbohydr. Polym.* **2016**, *151*, 160.
[20] D. P. Ferreira, D. S. Conceição, F. Fernandes, T. Sousa, R. C. Calhelha, I. C. F. R. Ferreira, P. F. Santos, L. F. Vieira Ferreira, *J. Phys. Chem. B* **2016**, *120*, 1212.
[21] J. F. Coelho, P. C. Ferreira, P. Alves, R. Cordeiro, A. C. Fonseca, J. R. Góis, M. H. Gil, *EPMA J.* **2010**, *1*, 164.
[22] W.-C. Lin, I.-T. Yeh, E. Niyama, W.-R. Huang, M. Ebara, C.-S. Wu, *Polymers* **2018**, *10*, 231.
[23] J. K. Patra, G. Das, L. F. Fraceto, E. V. R. Campos, M. D. P. Rodriguez-Torres, L. S. Acosta-Torres, L. A. Diaz-Torres, R. Grillo, M. K. Swamy, S. Sharma, S. Habtemariam, H.-S. Shin, *J. Nanobiotechnology* **2018**, *16*, 71.
[24] N. Goonoo, A. Bhaw-Luximon, D. Jhurry, *J. Biomed. Nanotechnol.* **2014**, *10*, 2173.
[25] Y. Fu, X. Li, Z. Ren, C. Mao, G. Han, *Small* **2018**, *14*, 1801183.
[26] D. Han, R. Serra, N. Gorelick, U. Fatima, C. G. Eberhart, H. Brem, B. Tyler, A. J. Steckl, *Sci. Rep.* **2019**, *9*, 17936.
[27] S. Chen, R. Li, X. Li, J. Xie, *Adv. Drug Delivery Rev.* **2018**, *132*, 188.
[28] A. D. Juncos Bombin, N. J. Dunne, H. O. Mccarthy, *Mater. Sci. Eng., C* **2020**, *114*, 110994.
[29] A. Memic, T. Abudula, H. S. Mohammed, K. Joshi Navare, T. Colombani, S. A. Bencherif, *ACS Appl. Bio Mater.* **2019**, *2*, 952.
[30] S. Wang, X. Wang, L. Yu, M. Sun, *Photodiagn. Photodyn. Ther.* **2021**, *34*, 102254.
[31] M. R. Hamblin, *Photochem. Photobiol.* **2020**, *96*, 506.
[32] H. Abrahamse, M. R. Hamblin, *Biochem. J.* **2016**, *473*, 347.
[33] S. W. Yoo, G. Oh, J. C. Ahn, E. Chung, *Biomedicines* **2021**, *9*, 113.
[34] V. A. Svyatchenko, S. D. Nikonov, A. P. Mayorov, M. L. Gelfond, V. B. Loktev, *Photodiagn. Photodyn. Ther.* **2021**, *33*, 102112.
[35] N. Kipshidze, N. Yeo, N. Kipshidze, *Nat. Photonics* **2020**, *14*, 651.
[36] S. Law, C. Lo, J. Han, A. W. Leung, C. Xu, *Photodiagn. Photodyn. Ther.* **2021**, *34*, 102284.
[37] J. Ghorbani, D. Rahban, S. Aghamiri, A. Teymouri, A. Bahador, *Laser Ther.* **2018**, *27*, 293.
[38] C. Donohoe, M. O. Senge, L. G. Arnaut, L. C. Gomes-Da-Silva, *Biochim. Biophys. Acta, Rev. Cancer* **2019**, *1872*, 188308.
[39] U. Chilakamarthi, L. Giribabu, *Chem. Rec.* **2017**, *17*, 775.
[40] M. R. Hamblin, *Dalton Trans.* **2018**, *47*, 8571.
[41] S. Kwiatkowski, B. Knap, D. Przystupski, J. Saczko, E. Kędzierska, K. Knap-Czop, J. Kotlińska, O. Michel, K. Kotowski, J. Kulbacka, *Biomed. Pharmacother.* **2018**, *106*, 1098.
[42] T. M. Tsubone, W. K. Martins, C. Pavani, H. C. Junqueira, R. Itri, M. S. Baptista, *Sci. Rep.* **2017**, *7*, 6734.
[43] S. M. Mahalingam, J. D. Ordaz, P. S. Low, *ACS Omega* **2018**, *3*, 6066.
[44] A. P. Castano, T. N. Demidova, M. R. Hamblin, *Photodiagn. Photodyn. Ther.* **2005**, *2*, 25048553.
[45] J. F. Algorri, M. Ochoa, P. Roldán-Varona, L. Rodríguez-Cobo, J. M. López-Higuera, *Cancers* **2021**, *13*, 4447.
[46] T. Suzuki, M. Tanaka, M. Sasaki, H. Ichikawa, H. Nishie, H. Kataoka, *Cancers* **2020**, *12*, 2369.
[47] E. Reginato, P. Wolf, M. R. Hamblin, *World J. Immunol.* **2014**, *4*, 25364655.
[48] A. Mohammadi, M. A. Doustvandi, M. R. Hamblin, *Photodiagn. Photodyn. Ther.* **2019**, *26*, 395.
[49] D. Conceição, D. Ferreira, L. Ferreira, *Int. J. Mol. Sci.* **2013**, *14*, 18557.
[50] A. Escudero, C. Carrillo-Carrión, M. C. Castillejos, E. Romero-Ben, C. Rosales-Barrios, N. Khiar, *Mater. Chem. Front.* **2021**, *5*, 3788.
[51] E. Lima, O. Ferreira, J. F. Silva, A. O. Santos, R. E. Boto, J. R. Fernandes, P. Almeida, S. M. Silvestre, L. V. Reis, L. V. Reis, *Dyes Pigm.* **2020**, *174*, 108024.
[52] D. P. Ferreira, D. S. Conceicao, V. R. A. Ferreira, V. C. Graca, P. F. Santos, L. F. Vieira Ferreira, *Photochem. Photobiol. Sci.* **2013**, *12*, 1948.
[53] X. Wang, D. Luo, J. P. Basilion, *Cancers* **2021**, *13*, 2992.
[54] I. S. Mfouo-Tynga, L. D. Dias, N. M. Inada, C. Kurachi, *Photodiagn. Photodyn. Ther.* **2021**, *34*, 102091.
[55] A. Luraghi, F. Peri, L. Moroni, *J. Controlled Release* **2021**, *334*, 463.
[56] M. Khodadadi, S. Alijani, M. Montazeri, N. Esmaeilizadeh, S. Sadeghi-Soureh, Y. Pilehvar-Soltanahmadi, *J. Biomed. Mater. Res., Part A* **2020**, *108*, 1444.
[57] Y. Ding, W. Li, F. Zhang, Z. Liu, N. Z. Ezazi, D. Liu, H. A. Santos, *Adv. Funct. Mater.* **2019**, *29*, 1802852.
[58] Q. Zhang, Y. Li, Z. Y. (William) Lin, K. K. Y. Wong, M. Lin, L. Yildirimer, X. Zhao, *Drug Discovery Today* **2017**, *22*, 1351.
[59] W.-Y. Huang, T. Hibino, S.-I. Suye, S. Fujita, *RSC Adv.* **2021**, *11*, 5703.
[60] C. Dhand, N. Dwivedi, H. Sriram, S. Bairagi, D. Rana, R. Lakshminarayanan, M. Ramalingam, S. Ramakrishna, in *Nanofiber Composites for Biomedical Applications* (Eds: M. Ramalingam, S. Ramakrishna), Woodhead Publishing, Cambridge **2017**, Ch. 8.

[61] Y. Ma, X. Wang, S. Zong, Z. Zhang, Z. Xie, Y. Huang, Y. Yue, S. Liu, X. Jing, *RSC Adv.* **2015**, *5*, 106325.
[62] D. Puppi, F. Chiellini, in *Woodhead Publ. Ser. Biomater.* (Eds: M. L. Focarete, T. Tampieri), Woodhead Publishing, Cambridge **2018**, Ch. 12.
[63] F. Serio, A. F. Da Cruz, A. Chandra, C. Nobile, G. R. Rossi, E. D'amone, G. Gigli, L. L. Del Mercato, C. C. De Oliveira, *Int. J. Biol. Macromol.* **2021**, *188*, 764.
[64] S. Kajdič, O. Planinšek, M. Gašperlin, P. Kocbek, *J. Drug Delivery Sci. Technol.* **2019**, *51*, 672.
[65] S. Abid, T. Hussain, Z. A. Raza, A. Nazir, *Mater. Sci. Eng., C* **2019**, *97*, 966.
[66] M. Afshari, in *Woodhead Publishing Series in Textiles* (Ed: M. Afshari), Woodhead Publishing, Cambridge **2017**, Ch. 1.
[67] R. Asmatulu, W. Khan, in *Micro Nano Technologies* (Eds: R. Asmatulu, W. S. Khan), Elsevier, Amsterdam **2019**, Ch. 2.
[68] K. Zhao, S.-X. Kang, Y.-Y. Yang, D.-G. Yu, *Polymers* **2021**, *13*, 226.
[69] G. I. Taylor, M. D. Van Dyke, *Proc. R. Soc. London, Ser. A* **1969**, *313*, 453.
[70] C. J. Luo, S. D. Stoyanov, E. Stride, E. Pelan, M. Edirisinghe, *Chem. Soc. Rev.* **2012**, *41*, 4708.
[71] J. Xue, T. Wu, Y. Dai, Y. Xia, *Chem. Rev.* **2019**, *119*, 5298.
[72] S. M. Costa, L. Pacheco, W. Antunes, R. Vieira, N. Bem, P. Teixeira, R. Fangueiro, D. P. Ferreira, *Appl. Sci.* **2022**, *12*, 67.
[73] F. Fadil, N. D. N. Affandi, M. I. Misnon, N. N. Bonnia, A. M. Harun, M. K. Alam, *Polymers* **2021**, *13*, 2087.
[74] Y.-Z. Long, X. Yan, X.-X. Wang, J. Zhang, M. Yu, in *Micro Nano Technologies* (Eds: B. Ding, X. Wang, J. Yu), William Andrew Publishing, Norwich, NY **2019**, Ch. 2.
[75] L. Wang, C. Zhang, F. Gao, G. Pan, *RSC Adv.* **2016**, *6*, 105988.
[76] A. S. Ribeiro, S. M. Costa, D. P. Ferreira, R. C. Calhelha, L. Barros, D. Stojković, M. Soković, I. C. F. R. Ferreira, R. Fangueiro, *React. Funct. Polym.* **2021**, *159*, 104808.
[77] U. M. Akpan, M. Pellegrini, J. D. Obayemi, T. Ezenwafor, D. Browl, C. J. Ani, D. Yiporo, A. Salifu, S. Dozie-Nwachukwu, S. Odusanya, J. Freeman, W. O. Soboyejo, *Mater. Sci. Eng., C* **2020**, *114*, 110976.
[78] L. Steffens, A. M. Morás, P. R. Arantes, K. Masterson, Z. Cao, M. Nugent, D. J. Moura, *Eur. J. Pharm. Sci.* **2020**, *143*, 105183.
[79] D. Han, M. Sasaki, H. Yoshino, S. Kofuji, A. T. Sasaki, A. J. Steckl, *J. Drug Delivery Sci. Technol.* **2017**, *40*, 45.
[80] E. Yan, Y. Fan, Z. Sun, J. Gao, X. Hao, S. Pei, C. Wang, L. Sun, D. Zhang, *Mater. Sci. Eng., C* **2014**, *41*, 217.
[81] L.-F. Zhu, Y. Zheng, J. Fan, Y. Yao, Z. Ahmad, M.-W. Chang, *Eur. J. Pharm. Sci.* **2019**, *137*, 105002.
[82] B. Darbasizadeh, S. A. Mortazavi, F. Kobarfard, M. R. Jaafari, A. Hashemi, H. Farhadnejad, B. Feyzi-Barnaji, *J. Drug Delivery Sci. Technol.* **2021**, *64*, 102576.
[83] A. S. Ribeiro, S. M. Costa, D. P. Ferreira, H. Abidi, R. Fangueiro, *Key Eng. Mater.* **2021**, *893*, 45.
[84] F. K. Mwiiri, R. Daniels, *Molecules* **2020**, *25*, 4799.
[85] P. Francavilla, D. P. Ferreira, J. C. Araújo, R. Fangueiro, *Appl. Sci.* **2021**, *11*, 1124.
[86] A. Haider, S. Haider, I.-K. Kang, *Arab. J. Chem.* **2018**, *11*, 1165.
[87] L. Wang, H. Yang, J. Hou, W. Zhang, C. Xiang, L. Li, *New J. Chem.* **2017**, *41*, 15072.
[88] W. Zuo, M. Zhu, W. Yang, H. Yu, Y. Chen, Y. Zhang, *Polym. Eng. Sci.* **2005**, *45*, 704.
[89] R. Khajavi, M. Abbasipour, in *Woodhead Publishing Series in Textiles* (Ed: M. Afshari), Woodhead Publishing, Cambridge **2017**, Ch. 5.
[90] M. M. Mahmud, A. Perveen, M. A. Matin, M. T. Arafat, *Mater. Res. Express* **2018**, *5*, 115407.
[91] F. Yalcinkaya, B. Yalcinkaya, O. Jirsak, in *Electrospinning – Material, Techniques, and Biomedical Applications* (Eds: S. Haider, A. Haider), IntechOpen, London **2016**.
[92] S. Huan, G. Liu, G. Han, W. Cheng, Z. Fu, Q. Wu, Q. Wang, *Materials* **2015**, *8*, 2718.
[93] A. Rajak, D. A. Hapidin, F. Iskandar, M. M. Munir, K. Khairurrijal, K. Khairurrijal, *Nanotechnology* **2019**, *30*, 425602.
[94] Y. Xu, L. Zou, H. Lu, T. Kang, *RSC Adv.* **2017**, *7*, 4000.
[95] S. Mondal, *Polym. Adv. Technol.* **2014**, *25*, 179.
[96] V. Pillay, C. Dott, Y. E. Choonara, C. Tyagi, L. Tomar, P. Kumar, L. C. du Toit, V. M. K. Ndesendo, *J. Nanomater.* **2013**, *2013*, 789289.
[97] Y. Sun, S. Cheng, W. Lu, Y. Wang, P. Zhang, Q. Yao, *RSC Adv.* **2019**, *9*, 25712.
[98] S. Haghju, M. R. Bari, M. A. Khaled-Abad, *Carbohydr. Polym.* **2018**, *200*, 137.
[99] Y. Bagbi, A. Pandey, P. R. Solanki, in *Micro Nano Technologies* (Eds: S. Thomas, D. Pasquini, S.-Y. Leu, D. A. Gopakumar), Elsevier, Amsterdam **2019**, Ch. 10.
[100] A. S. Motamedi, H. Mirzadeh, F. Hajiesmaeilbaigi, S. Bagheri-Khoulenjani, M. Shokrgozar, *Prog. Biomater.* **2017**, *6*, 113.
[101] L. A. Can-Herrera, A. I. Oliva, M. A. A. Dzul-Cervantes, O. F. Pacheco-Salazar, J. M. Cervantes-Uc, *Polymers* **2021**, *13*, 662.
[102] S. Zargham, S. Bazgir, A. Tavakoli, A. S. Rashidi, R. Damerchely, *J. Eng. Fiber. Fabr.* **2012**, *7*, 155892501200700400.
[103] C. Ribeiro, V. Sencadas, C. M. Costa, J. L. Gómez Ribelles, S. Lanceros-Méndez, *Sci. Technol. Adv. Mater.* **2011**, *12*, 015001.
[104] P. P. Mehta, V. S. Pawar, in *Woodhead Publishing Series in Biomaterials* (Eds: A. M. A. Inamuddin, A. Mohammad), Woodhead Publishing, Cambridge **2018**, Ch. 22.
[105] K. P. Matabola, R. M. Moutloali, *J. Mater. Sci.* **2013**, *48*, 5475.
[106] B. Abunahel, N. N. Azman, M. Jamil, *Chem. Mater. Eng.* **2018**, *12*, 296.
[107] H. He, Y. Kara, K. Molnar, *Resolut. Discovery* **2019**, *4*, 7.
[108] M. A. Alfaro De Prá, R. M. Ribeiro-Do-Valle, M. Maraschin, B. Veleirinho, *Mater. Lett.* **2017**, *193*, 154.
[109] J. Pelipenko, J. Kristl, B. Janković, S. Baumgartner, P. Kocbek, *Int. J. Pharm.* **2013**, *456*, 125.
[110] R. Ghobeira, M. Asadian, C. Vercruysse, H. Declercq, N. De Geyter, R. Morent, *Polymer* **2018**, *157*, 19.
[111] L. Tijing, Y. C. Woo, M. Yao, J. Ren, H. K. Shon, in *Reference Module in Chemistry, Molecular Sciences and Chemical Engineering*, Vol. 1 (Eds: E. Drioli, L. Giorno, E. Fontananova), Elsevier, Amsterdam **2017**, Ch. 1.16.
[112] S. De Vrieze, T. Van Camp, A. Nelvig, B. Hagström, P. Westbroek, K. De Clerck, *J. Mater. Sci.* **2009**, *44*, 1357.
[113] G.-Z. Yang, H.-P. Li, J.-H. Yang, J. Wan, D.-G. Yu, *Nanoscale Res. Lett.* **2017**, *12*, 55.
[114] E. Tamariz, A. Rios-Ramirez, in *Biodegradation – Life of Science* (Eds: R. Chamy, F. Rosenkranz), IntechOpen, London **2013**.
[115] R. De Souza, P. Zahedi, C. J. Allen, M. Piquette-Miller, *Drug Delivery* **2010**, *17*, 365.
[116] F. Asghari, M. Samiei, K. Adibkia, A. Akbarzadeh, S. Davaran, *Artif. Cells Nanomed., Biotechnol.* **2017**, *45*, 185.
[117] A. Hivechi, S. H. Bahrami, R. A. Siegel, *Mater. Sci. Eng., C* **2019**, *94*, 929.
[118] M. V. Vellayappan, J. R. Venugopal, S. Ramakrishna, S. Ray, A. F. Ismail, M. Mandal, A. Manikandan, S. Seal, S. K. Jaganathan, *RSC Adv.* **2016**, *6*, 83638.
[119] H. Begum, M. K. R. Khan, *Int. J. Text. Sci.* **2017**, *6*, 110.
[120] J. Wang, M. Windbergs, *Eur. J. Pharm. Sci.* **2018**, *124*, 71.
[121] M. A. Teixeira, M. T. P. Amorim, H. P. Felgueiras, *Polymers* **2019**, *12*, 7.
[122] S. Shahriar, J. Mondal, M. Hasan, V. Revuri, D. Lee, Y.-K. Lee, *Nanomaterials* **2019**, *9*, 532.
[123] D.-G. Yu, X.-F. Zhang, X.-X. Shen, C. Brandford-White, L.-M. Zhu, *Polym. Int.* **2009**, *58*, 1010.
[124] X. Qin, in *Woodhead Publishing Series in Textiles* (Ed: M. Afshari), Woodhead Publishing, Cambridge **2017**, Ch. 3.
[125] M. F. Abdullah, T. Nuge, A. Andriyana, B. C. Ang, F. Muhamad, *Polym.* **2019**, *11*, 2008.

[126] B. Pant, M. Park, S.-J. Park, *Pharmaceutics* **2019**, *11*, 305.
[127] M. Nasari, D. Semnani, M. Hadjianfar, S. Amanpour, *J. Mater. Sci.* **2020**, *55*, 10185.
[128] M. Buzgo, A. Mickova, M. Rampichova, M. Doupnik, in *Woodhead Publishing Series in Biomaterials* (Eds: M. L. Focarete, A. Tampieri), Woodhead Publishing, Cambridge **2018**, Ch. 11.
[129] N. Nikmaram, S. Roohinejad, S. Hashemi, M. Koubaa, F. J. Barba, A. Abbaspourrad, R. Greiner, *RSC Adv.* **2017**, *7*, 28951.
[130] M. Liu, X. Hao, Y. Wang, Z. Jiang, H. Zhang, *J. Mater. Sci.* **2020**, *55*, 16730.
[131] B. Niemczyk-Soczynska, A. Gradys, P. Sajkiewicz, *Polymers* **2020**, *12*, 2636.
[132] H. Amani, H. Arzaghi, M. Bayandori, A. S. Dezfuli, H. Pazoki-Toroudi, A. Shafiee, L. Moradi, *Adv. Mater. Interfaces* **2019**, *6*, 1900572.
[133] J. Wu, Z. Zhang, J. G. Gu, W. Zhou, X. Liang, G. Zhou, C. C. Han, S. Xu, Y. Liu, *J. Controlled Release* **2020**, *320*, 337.
[134] Q. Zhang, Z. Lin, W. Zhang, T. Huang, J. Jiang, Y. Ren, R. Zhang, W. Li, X. Zhang, Q. Tu, *RSC Adv.* **2021**, *11*, 1012.
[135] J. Yoo, Y.-Y. Won, *ACS Biomater. Sci. Eng.* **2020**, *6*, 6053.
[136] F. Moradi Kashkooli, M. Soltani, M. Souri, *J. Controlled Release* **2020**, *327*, 316.
[137] R. Ramachandran, V. R. Junnuthula, G. S. Gowd, A. Ashokan, J. Thomas, R. Peethambaran, A. Thomas, A. K. K. Unni, D. Panikar, S. V. Nair, M. Koyakutty, *Sci. Rep.* **2017**, *7*, 43271.
[138] X. Liu, W. Zhang, Y. Wang, Y. Chen, J. Xie, J. Su, C. Huang, *J. Controlled Release* **2020**, *320*, 201.
[139] D. Kharaghani, P. Gitigard, H. Ohtani, K. O. Kim, S. Ullah, Y. Saito, M. Q. Khan, I. S. Kim, *Sci. Rep.* **2019**, *9*, 12640.
[140] M. Alishahi, M. Khorram, Q. Asgari, F. Davani, F. Goudarzi, A. Emami, A. Arastehfar, K. Zomorodian, *Int. J. Biol. Macromol.* **2020**, *163*, 288.
[141] M. Maleki, M. Latifi, M. Amani-Tehran, S. Mathur, *Polym. Eng. Sci.* **2013**, *53*, 1770.
[142] T. Abudula, K. Gauthaman, A. Mostafavi, A. Alshahrie, N. Salah, P. Morganti, A. Chianese, A. Tamayol, A. Memic, *Sci. Rep.* **2020**, *10*, 20428.
[143] Y. Yang, S. Chang, Y. Bai, Y. Du, D.-G. Yu, *Carbohydr. Polym.* **2020**, *243*, 116477.
[144] S. Wen, Y. Hu, Y. Zhang, S. Huang, Y. Zuo, Y. Min, *Mater. Sci. Eng., C* **2019**, *100*, 514.
[145] F. Rahmani, H. Ziyadi, M. Baghali, H. Luo, S. Ramakrishna, *Appl. Sci.* **2021**, *11*, 2779.
[146] V. Agrahari, V. Agrahari, J. Meng, A. K. Mitra, in *Micro Nano Technologies* (Eds: A. K. Mitra, K. Cholkar, A. Mandal), Elsevier, Boston, MA **2017**, Ch. 9.
[147] H.-M. Wu, N. Chen, Z.-M. Wu, Z.-L. Chen, Y.-J. Yan, *J. Biomater. Appl.* **2013**, *27*, 773.
[148] F. Ma, C.-W. Yuan, X.-X. Ren, C.-J. You, J.-H. Cao, D.-Y. Wu, *J. Photochem. Photobiol., A* **2018**, *355*, 267.
[149] A. N. Severyukhina, N. V. Petrova, K. Smuda, G. S. Terentyuk, B. N. Klebtsov, R. Georgieva, H. Bäumler, D. A. Gorin, *Colloids Surf., B* **2016**, *144*, 57.
[150] J. J. Yoo, C. Kim, C.-W. Chung, Y.-I. Jeong, D. H. Kang, *Int. J. Nanomed.* **2012**, *7*, 1997.
[151] J. Xiao, L. Cheng, T. Fang, Y. Zhang, J. Zhou, R. Cheng, W. Tang, X. Zhong, Y. Lu, L. Deng, Y. Cheng, Y. Zhu, Z. Liu, W. Cui, *Small* **2019**, *15*, 1904979.
[152] F. Cieplik, D. Deng, W. Crielaard, W. Buchalla, E. Hellwig, A. Al-Ahmad, T. Maisch, *Crit. Rev. Microbiol.* **2018**, *44*, 571.
[153] H. Samadian, S. Zamiri, A. Ehterami, S. Farzamfar, A. Vaez, H. Khastar, M. Alam, A. Ai, H. Derakhshankhah, Z. Allahyari, A. Goodarzi, M. Salehi, *Sci. Rep.* **2020**, *10*, 8312.
[154] H. Qiu, S. Zhu, L. Pang, J. Ma, Y. Liu, L. Du, Y. Wu, Y. Jin, *Int. J. Pharm.* **2020**, *588*, 119797.
[155] T. Czapka, A. Winkler, I. Maliszewska, R. Kacprzyk, *Energies* **2021**, *14*, 2598.
[156] A. Contreras, M. J. Raxworthy, S. Wood, J. D. Schiffman, G. Tronci, *ACS Appl. Bio Mater.* **2019**, *2*, 4258.
[157] E. Preis, T. Anders, J. Širc, R. Hobzova, A.-I. Cocarta, U. Bakowsky, J. Jedelská, *Mater. Sci. Eng., C* **2020**, *115*, 111068.
[158] S. Jiang, B. C. Ma, W. Huang, A. Kaltbeitzel, G. Kizisavas, D. Crespy, K. A. I. Zhang, K. Landfester, *Nanoscale Horiz.* **2018**, *3*, 439.
[159] J. Dong, R. A. Ghiladi, Q. Wang, Y. Cai, Q. Wei, *Nanotechnology* **2018**, *29*, 265601.
[160] L. El-Khordagui, N. El-Sayed, S. Galal, H. El-Gowelli, H. Omar, M. Mohamed, *Int. J. Pharm.* **2017**, *520*, 139.
[161] L. Sun, L. Song, X. Zhang, R. Zhou, J. Yin, S. Luan, *Mater. Sci. Eng., C* **2020**, *113*, 110936.
[162] S. Qian, L. Song, L. Sun, X. Zhang, Z. Xin, J. Yin, S. Luan, *J. Photochem. Photobiol., A* **2020**, *400*, 112626.
[163] C.-L. Liu, J. Yang, X.-H. Bai, Z.-K. Cao, C. Yang, S. Ramakrishna, D.-P. Yang, J. Zhang, Y.-Z. Long, *Nanoscale Res. Lett.* **2021**, *16*, 54.
[164] J. Zhang, C.-L. Liu, J.-J. Liu, X.-H. Bai, Z.-K. Cao, J. Yang, M. Yu, S. Ramakrishna, Y.-Z. Long, *Nanoscale* **2021**, *13*, 6105.

Sofia M. Costa is a Ph.D. student at Centre for Textile Science and Technology (2C2T) from the University of Minho (SFRH/BD/147517/2019). Her main research focuses on the development of local drug delivery systems based on electrospun nanofibers using biodegradable polymers for cancer photodynamic therapy.

Raul Fangueiro is Cathedratic Professor at Centre for Textile Science and Technology (2C2T) from the University of Minho and he is also the director of this center. His main research is focused on fiber-based materials, nanofibers produced by electrospinning, multiscale composites, functionally graded composites, and composites for defense.

Diana P. Ferreira is presently junior researcher at Centre for Textile Science and Technology (2C2T) from the University of Minho. She holds a doctoral degree in chemistry at Instituto Superior Técnico. Her main research is focus on CBRN protective materials, electrospun nanofibers, natural fibers, functionalization of fibrous structures, synthesis of nanoparticles, piezoresistive materials, localized drug delivery systems, wound dressing systems, and photodynamic therapy.